DEVELOPMENT OF AN OPTICAL BIOSENSOR FOR URIC ACID DETERMINATION

A Thesis

by

TOKUNBO SAID FALOHUN

Submitted to the Office of Graduate and Professional Studies of
Texas A&M University
in partial fulfillment of the requirements for the degree of

MASTER OF SCIENCE

Chair of Committee,	Mike McShane
Committee Members,	Melissa Grunlan
	Gerard Coté
Head of Department,	Mike McShane

December 2019

Major Subject: Biomedical Engineering

ABSTRACT

Affordable, accessible biosensors for the diagnosis, management, and treatment of chronic diseases are critical to reducing healthcare costs. An often overlooked chronic condition that affects over 8 million Americans is gout. This condition is characterized by severe pain, and in more advanced cases, bone erosion and joint destruction. This thesis explores the fabrication and characterization of an optical, enzymatic uric acid biosensor for gout management, and the optimization of the biosensor response through the tuning of hydrogel matrix properties.

Sensors were fabricated through the co-immobilization of oxygen-quenched phosphorescent probes with oxidoreductases within a biocompatible copolymer hydrogel matrix. Characterization of spectral properties and hydrogel swelling was conducted. In addition, evaluations of the sensitivity, repeatability, and long-term stability of the uric acid biosensor were conducted. The findings indicate that increased acrylamide concentration improved the biosensor response by yielding increased sensitivity and reduced lower limit of detection. However, the repeatability and stability tests highlighted some possible areas of improvement. Specifically, a consistent drift was observed in the response during repeatability testing, and a reduction in sensor response was seen after long-term storage tests. Overall, this study demonstrates the potential of an on-demand, patient-friendly gout management tool. This work also demonstrates an alternate use of the porphyrin-oxidoreductase biosensing platform and paves the way for a multi-analyte biosensor.

DEDICATION

This work is dedicated to my cousin, Toyyib Abib, who recently passed away at the young age of 15. Loved and respected by hundreds in his community, he had dreams of studying biomedical engineering before embarking on a career as a neurosurgeon. Toyyib was full of life and promise. His passion was contagious, and for a boy his age, he demonstrated extraordinary curiosity and ambition. Although he is no longer physically here to realize those dreams, his soul lives in those that had the privilege of knowing him. An invaluable lesson I picked up from Toyyib was to have the courage to dream big, even when confronted with fear. He will be forever missed but never forgotten.

ACKNOWLEDGEMENTS

I would like to thank my committee chair, Dr. McShane, and my committee members, Dr. Grunlan, and Dr. Coté for their guidance and support throughout the course of this research. My current lab group members have played a pivotal role in the development of my skills as thinker and researcher. Former members of the BioSyM have also played an essential role in paving the way for this work, particularly Rachel Unruh, Lindsey Harris, and Liam Andrus. Finally, I would like to thank my friends and family, in Texas and Maryland, for the continued support through the duration of my master's degree.

CONTRIBUTORS AND FUNDING SOURCES

Contributors

This work was supervised by a thesis committee consisting of Professor Michael McShane, Melissa Grunlan, and Gerard Coté of the Department of Biomedical Engineering

The porphyrin dye used for biosensor fabrication was donated by PROFUSA Inc., (San Francisco, CA).

All work conducted for the thesis was completed by the student independently.

Funding Sources

Graduate study was supported by the Louis Stokes Alliance for Minority Participation Bridge to Doctorate Fellowship Program fellowship and the Diversity Fellowship by the Office of Graduate and Professional Studies by Texas A&M University. This work was in part supported by the National Institutes of Health (#1R01EB024601). The contents presented herein solely represent the views of the author and do not represent that of the National Institutes of Health.

NOMENCLATURE

AAm	Acrylamide
AEMA	2-aminoethylmethacrylate
BMAP	Palladium (II) tetramethacrylated Benzoporphyrin
DI Water	Deionized water
DMSO	Dimethyl sulfoxide
EDC	1-ethyl-3-(3-dimethylamino) propyl carbodiimide hydrochloride
EGDMA	Ethylene glycol dimethacrylate
HEMA	2-Hydroxyethyl Methacrylate
NHS	N-hydroxysuccinimide
PBS	Phosphate-buffered saline
PdBP	Tetramethacrylated Pd(II) benzoporphyrin
PEG	Poly(ethylene glycol)
TEGDMA	Tetraethylene glycol dimethacrylate
λ_{ex}	Excitation wavelength
λ_{em}	Excitation wavelength

TABLE OF CONTENTS

LIST OF FIGURES

LIST OF TABLES

Page

1. INTRODUCTION

1.1 The Chronic Disease Epidemic

Advancements in science, medicine, sanitation and public health infrastructure over the past century has led to a surge in the average American lifespan from 47 years in 1900 to 79 years in 2010.[1] According to the US Census Bureau, the percentage of the population 65 years and above has doubled within the past 50 years and is expected to continue to increase in the upcoming decades.[2] This increase in lifespan marks one of the greatest human achievements, largely attributed to the reduction of infectious diseases and infant death.[1] However, while the mortality from infectious diseases, such as tuberculosis and pneumonia, have significantly reduced, chronic illnesses like heart disease, cancer, respiratory disease, and diabetes have emerged as the leading causes of death in the world and are becoming increasingly prevalent as the world's population continues to age.[3]

Due to rising healthcare costs, expanding population, and growing shortage of nurses and physicians, most healthcare systems are not well suited to handle this rising burden of chronic diseases.[4] According to the World Health Organization, chronic diseases constitute of 78% of all medical expenses in the United States,[5] and 18% of the GDP.[6] Even more alarming is that just 5% of the most severely chronically ill patients account for over half of all healthcare expenditures.[7] Contrary to popular belief, the burden of chronic diseases is perhaps even more detrimental in developing nations, which are simultaneously affected by infectious and chronic diseases, while being hindered by the lack of resources and poor healthcare infrastructure.[8] India for instance, has the largest diabetic population in the world,[9] while suffering from high mortality rates from malaria and pneumonia.[10] South Africa, and many other developing nations are undergoing a similar

epidemiological transition.[11] Clearly, the rise of chronic diseases is one of the largest global issues we currently face.

The need for affordable, accessible options for the diagnosis, management, and treatment of patients at risk or suffering from chronic diseases is critical to reducing healthcare costs and improving living standards of millions worldwide. This concern has fueled intense research in fields like pharmacology, genetics, radiology, data analytics, biomaterials, tissue engineering, and drug delivery. The field of biosensors, which are analytical tools capable of converting biological events into measurable signals, has also become an area of strong interest as tools in precision medicine[12] and mobile health (mHealth)[13] capable of providing low-cost but accurate patient health information without exhausting expensive clinical labor and facilities. As such, the market biosensors is projected to reach $21 billion dollars by 2020.[14]

1.2 An Overview of Biosensors

The study of biosensors has become a vast, interdisciplinary field, spanning a wide variety of disciples, including chemistry, physics, and biology among others.[15] Due to the wide number of applications in fields like agriculture, nutritional science, defense, environmental science, and medicine, biosensors have sparked the interests of researchers both in academia and industry. Examples of commercially available biosensors used in medical applications include glucose test strips for diabetes management and pregnancy tests.

Biosensors differ from physical sensors, which measure physical parameters, such as respiratory rate, heart rate (pulse), electrocardiogram (ECG), blood pressure, body temperature, and oxygen saturation level.[16] These parameters are usually measured using miniaturized electrodes, LEDs, and photodiodes embedded in a skin-interfacing wearable, such as smart watches, patches, smart tattoos.[17] Due to advancements in processing power and wireless

communications, numerous consumer devices with physical sensing capabilities, like the Apple Watch, Fitbit, and Samsung Gear have reached the market and seen widespread adoption.[18] Many of these devices primarily focus on fitness and general wellness purposes, unlike biosensors which tend to be medical devices focused on disease management through the detection of chemical substances in the body.

Biosensors are primarily composed of two components (Figure 1-1): (1) a biorecognition element that specifically detects the target analyte of interest, and (2) a signal transducer that converts the detection of the analyte into a measurable signal. Other significant components include the signal processor and scaffold to immobilize the sensing components.[19,20]

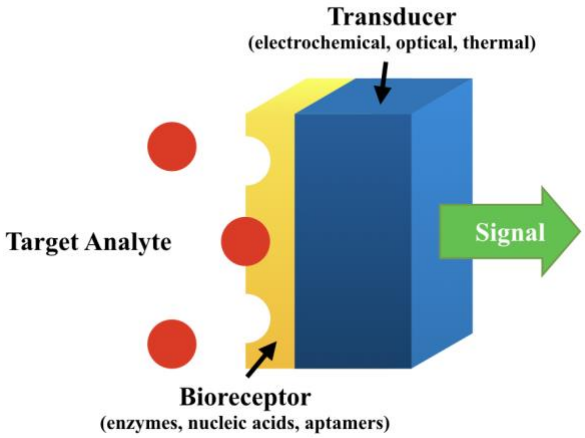

Figure 1-1: Schematic representation of a biosensor

Biosensors are often categorized by their method of signal transduction and by the mechanism of the biorecognition element. Methods of biorecognition include the use of enzymes, antibodies, nucleic acids, aptamers, nanoparticles, and cells.[21] Due to the exceptional selectivity naturally enabled by their unique 3D conformation and capability to efficiently catalyze certain chemical reactions, enzymes are the most widely used biorecognition molecules.[22] Common methods of signal transduction include optical, piezoelectric, thermal, magnetic, micromechanical,

and electrochemical techniques. Biosensors based on electrochemical signal transduction are currently the most common,[6] although optical modalities are also widely used.[15]

The first true biosensor, known as the glucose enzyme electrode, was pioneered by Leland Clark and Champ Lyons in 1962 and was of the electrochemical sort.[23] The glucose enzyme electrode, which built upon the Clark oxygen electrode discovered in 1959,[6,24] consisted of a platinum electrode, surrounded by a layer of glucose oxidase solution entrapped in a semipermeable membrane. The device indirectly detected glucose through the measurement of oxygen, which was consumed by glucose oxidase during the catalysis of glucose into gluconic acid and hydrogen peroxide.[25] Over a half century later, this mechanism of glucose biosensing has only been slightly modified, with hydrogen peroxide being detected instead of oxygen. The Clark enzyme electrode paved the way for the miniaturized disposable glucose-sensing strips and transcutaneous glucose biosensors widely used by diabetics today for the self-monitoring of blood glucose. These amperometric glucose sensors currently dominate the biosensor market, consisting of 85% of the global biosensor market due to the prevalence of diabetes mellitus in societies around the globe.[6]

Biosensors vary not only in their method of signal transduction and mechanism of analyte biorecognition, but in their form-factor and how they interact with biofluids or target analytes. Two promising biosensor configurations that eliminate the need for blood sampling are wearable and implantable biosensors.[17] Target biofluids for wearable biosensors include interstitial fluid, sweat, tears, and saliva.[26] Implantable biosensors on the other hand, primarily target blood, interstitial fluid, and cerebrospinal fluid.[27,28] Measurement of analytes in each of these biofluids presents a number of challenges, perhaps none greater than finding a correlation with serum analyte concentrations. Although the correlation between serum glucose concentration and

interstitial glucose concentration has been well established,[28,29] a similar correlation has not been established with other biofluids, or even between serum and interstitial fluid using other analytes. Consequently, this lack of established correlations between analyte concentrations in serum and alternate biofluids has been a limiting factor in the development of a wider variety of biosensors.[6,30,31]

Another challenge in developing wearable biosensors in particular is in obtaining reliable and adequate volume of biofluids samples.[32] A prominent example of this obstacle was seen in the GlucoWatch biographer by Cygnus Inc., which was the First FDA-approved non-invasive glucose biosensor (2001).[33] To obtain biofluid samples, this device used reverse iontophoresis (RI) where oppositely charged electrodes are used to pass a mild current through the skin to drive the electro-osmotic flow of metabolites, such as glucose and sodium, from the interstitial fluid to the surface of the skin. However, RI-induced skin irritation and inaccuracies in glucose readings lead to the removal of this device from the market.[26] Research on the development of contact-lens glucose biosensors by industry giants, like Google/Verily Life Sciences and Novartis, have also been derailed by similar challenges in consistently obtaining reliable biofluid samples (tears) with glucose concentrations that strongly correlation with serum glucose levels.[34]

Although currently elusive, establishing correlations between human serum and alternate biofluids can open the doors to the development of wearable biosensors that can be used in real-time monitoring of analytes in tears, sweat, interstitial fluid or saliva.[35] Non-invasive, wearable biosensors would not only be strongly desired by patients and physicians, but by society as a whole, as out-of-hospital patient health monitoring could potentially reduce costs incurred through hospital visits, while enabling better personalized care.[36]

1.3 Implantable Biosensors

By directly interfacing with human serum *in situ*, implantable biosensors circumvent many of the issues that affect the accuracy of wearable biosensors. Both of these biosensor types offer two key benefits. First is their ability to continuously monitor analytes, which allows patients to be notified when analyte levels cross dangerous thresholds that may not be captured through intermittent discrete monitoring. Continuous monitoring also provides the potential to better understand how analyte levels are affected by changes in diet, lifestyle habits, and medication.[37] The second key advantage of wearable and implantable biosensors is the flexibility and convenience they offer to patients and clinicians. Since implantable biosensors can passively perform analyte measurements, while requiring minimal intervention from physicians and patients, they can serve as excellent tools for remote patient monitoring, while improving patient compliance.

When compared to wearables, implantable biosensors are not without their challenges. Perhaps the most significant of these challenges is the effect of the foreign body response (FBR) on device biocompatibility, which refers to the ability of the biosensor to remain safe and effective throughout the operational lifetime of the device.[38] The foreign body response consists of a combination of acute and chronic inflammation. Acute inflammation occurs immediately after biosensor implantation and consists of the non-specific absorption of proteins such as albumin and fibrinogen to the surface of the implant.[39] During chronic inflammation, macrophages play a central role in the formation of foreign body giant cells, the release of enzymes and reactive oxygen species capable of degrading the implant, as well as in the recruitment of pro-fibrotic agents that lead to the formation of a fibrous capsule around the implant.[40] Therefore, considerations must be made during the design of implantable biosensors for (1) the reduction in analyte diffusion into

the biosensor matrix due to the formation of a fibrotic capsule around the biosensor implant, and (2) the local change in the physiological and chemical environment due to the acute and chronic inflammation. Despite these challenges, the potential of implantable biosensors in precision medicine and chronic disease management remains promising.

While several needle-based transcutaneous continuous glucose monitors (CGMs) exist, very few fully-implantable biosensors have been brought to the market. The CGMs currently on the market, which include the Medtronic Guardian, Dexcom G6 CGM, and Abbott FreeStyle Libre, must be replaced every 7-14 days and are incapable of long-term biosensing because they open up a pathway for infection, and exacerbate the foreign body response due to their mechanical incompatibility and recurring micromotion.[41-43]

Noteworthy is the Eversense long-term continuous glucose monitor by Senseonics, the first fully-implantable glucose biosensor.[44] In July 2018, the Food and Drug Administration granted a premarket approval of this 90-day implantable glucose biosensor. A larger, more robust version of the Eversense, known as the Eversense XL CGM, has been shown to last for twice as long, and received a CE Mark of approval for use in the EU in September 2017.[45] The functionality of the Eversense is based on boronic acid detection of glucose and fluorescent optical transduction. Interestingly, a 3-way comparison between the Eversense, Dexcom G5, and Abbott Freestyle Libre Pro found the Eversense to be "significantly better than two other CGM systems," when compared to measurements using a traditional glucose strip.[46] This may be due to the reduced foreign body response of a fully implanted system when compared to transcutaneous biosensors.

Despite the prevalence of implantable glucose biosensors, there exist numerous other biosensor applications for the management of chronic diseases. In fact, mortalities from heart diseases, cancer, and chronic lung diseases are roughly seventeen, seven, and four times greater

than that of diabetes, respectively.[3] Reducing the chronic disease burden therefore requires the exploration of other analytes during the development of novel biosensor technologies, with glucose biosensors serving as a possible model for the design and commercialization of such devices. As such, work is underway on identifying detectable biomarkers that can be used to monitor various disease states.[47-49] Thousands of biosensors for a wide range of analytes, much of which are outside the scope of this report, have been reported on.[50]

1.4 Research Objective

This thesis explores the systematic development and characterization of an optical, enzymatic uric acid biosensor for gout management. Measurements of uric acid levels would enable gout patients to monitor the dynamics of their uric acid concentrations, allowing them to take anti-hyperuricemic medication or make adjustments in their diet and water intake to reduce the risk of unexpected gout attacks. Sensors were fabricated through the co-immobilization of oxygen-quenched phosphorescent probes with an oxidoreductase within a biocompatible copolymer hydrogel matrix. The effect of the hydrogel composition on the swelling, oxygen sensitivity, and uric acid sensitivity was evaluated. To further evaluate the viability of this platform, the selectivity, short-term cyclic performance, and long-term stability of the system was tested. Building on previous studies by the McShane group, this study expands the applications of our sensing platform, beyond oxygen, glucose and lactate sensing that have been previously been studied.[51-53] Overall, the objective of this project is twofold: First, to develop a minimally-invasive biosensor for uric acid determination, which has substantial individual merit for gout management and second, to expand the utility of our sensing platform, thereby laying the foundation for the development of a multianalyte biosensor.

1.5 Outline of Sections

The following sections of this thesis include the: Background and Literature Review (Section 2), Materials and Methods (Section 3), Results and Discussion (Section 4), Summary and Conclusions (Section 5), and References. Section 2 provides the clinical motivation for uric acid biosensing and summarizes the relevant literature on current uric acid measurement techniques, highlighting the need for accessible, patient-friendly tools for uric acid measurement. Section 2 also reviews current biosensor technologies and explains the utility of an optical biosensor for chronic gout management. The section concludes with a description of the porphyrin-oxidoreductase platform as a novel tool for conducting *in-vivo* and *ex-vivo* uric acid measurements.

Section 3 details the materials, and experimental protocols used in the fabrication and characterization of the uric acid biosensors, while Section 4 presents the findings and analysis of the described experiments, with special emphasis on the comparison of the sensitivity between biosensor compositions. These complete set of experiments include: (1) spectral characterization of the excitation and emission of the porphyrin molecules immobilized in biosensor matrices, (2) swelling ratio experiments to quantify the hydrophilicity of the different hydrogel compositions, (3 and 4) oxygen and uric acid response tests to investigate the sensitivity of the system to oxygen and uric acid changes, (5) selectivity experiments involving the exposure of sensors to various analytes, and (6) long-term stability tests to investigate the longevity of the biosensing system.

Finally, Section 5 concludes the thesis by summarizing the notable findings and key takeaways from this work. This section also describes the major limitations of the system, with proposed solutions to several of these challenges. An outlook on future of this platform as a possible multianalyte biosensor is provided at the end of the section. References to numerous

published works that supported the experimentation and analysis contained in this report were also reported.

2. BACKGROUND AND LITERATURE REVIEW

2.1 Arthritis and Gout

Arthritis is one of the most prevalent chronic conditions in the United States, affecting over 21% of all U.S. adults and roughly 50% of adults 65 and above.[54] Despite not usually being fatal, the condition is a large economic burden to society and can dramatically reduce the quality of life of patients.[55] The term arthritis is actually loosely defined, and describes a range of over 100 rheumatic conditions. Some of the most prevalent forms of arthritis include osteoarthritis, rheumatoid arthritis, fibromyalgia and gout.[56] While each of these forms of arthritis have unique underlying causes, common symptoms they share are pain, swelling, and redness of the affected joint(s).

Gout is the most prevalent form of inflammatory arthritis,[57] affecting over 8 million individuals in the United States. Due to the aging population and poor dietary habits in society, this figure is only expected to increase in the upcoming decades.[58] Prevalent in elderly populations, gout is known as one of the most painful medical conditions suffered by humans and can severely limit the mobility of patients, inhibiting the freedom to pursue normal daily activities. Gout also presents a significant economic burden and those who suffer from the condition experience a $3000 average increase in annual healthcare and $1300 average increase in annual work-related expenses.[59,60]

2.2 Pathophysiology of Gout

Gout occurs due to the formation and accumulation of uric acid crystals around the joints.[61] Uric acid (Figure 2-1), is a heterocyclic compound found throughout the body and is the end-product of purine metabolism. Purines are derived from exogenous sources, such as seafood and

red meat. As well as endogenously from nucleoproteins revealed after cell death.[62,63] Uric acid is produced by the liver and excreted by the kidneys or gastrointestinal tract. The compound is a weak acid, with a pKa of 5.8.[61] Therefore, in physiological conditions, the compound mostly exists as its deprotonated resonance hybrid, urate, and associates with sodium ions to form monosodium urate (MSU) salts.[64]

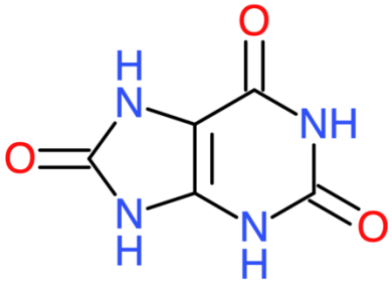

Figure 2-1: Chemical structure of uric acid

The supersaturation of uric acid in the blood stream occurs around 6.8 mg/dL, where uric acid reaches its physiological solubility limit in human plasma. In some cases, hyperuricemia leads to the deposition of urate crystals in the articular and periarticular tissue of the joints. The phagocytosis of these crystals by neutrophils induces an inflammatory response, which consists of a migration of leukocytes and the release of pro-inflammatory cytokines, which leads to swelling, severe pain (gout attack), and in more advanced chronic cases, bone erosion and destruction.[64,65]

An excruciating pain in the big toe during sleep is the hallmark of the onset of a gout attack. During one of these flares, the mere weight of one's bedsheets can lead to a severely painful throbbing sensation that is caused by the increased urate crystallization that tends to occur at cooler night-time temperatures.[66] Distal joints, particularly the first metatarsophalangeal joint of the big toe, is the region most affected by gout because of the lack of blood flow,[67] combined with the gravity-induced sinking of these crystals, due to their relatively high density, that leads to the increased accumulation of urate in this region.

Hence, the most prevalent risk factor for this crystal-induced inflammation is hyperuricemia,[58] which occurs when there is either an overproduction, or insufficient removal of uric acid from the blood stream by the kidneys. In 90% of hyperuricemia cases, insufficient renal excretion is the underlying factor.[65,68] Interestingly, most individuals (~78%) with hyperuricemia remain asymptomatic. However, the vast majority of patients who suffer from gout are hyperuricemic.[66]

Since humans, unlike most other mammals, lack the enzyme needed to break down the compound, an inability to excrete uric acid leads to a harmful accumulation of the compound in the body. Incidentally, the presence of estrogen in women is hypothesized to reduce urate deposition through the upregulation of renal excretion of the compound. Therefore, the risk of hyperuricemia is generally higher among men. Rates of hyperuricemia also rises significantly in older populations, likely due to a decrease in renal efficiency, although the exact reasons remain unclear.[65]

In addition to gout, hyperuricemia is also associated with several pathological conditions like renal insufficiency, Lesch–Nyhan syndrome, insulin resistance, leukemia, and nephrolithiasis.[61,69] Furthermore, patients undergoing chemotherapy or voluntary fasting in preparation of surgical anesthesia may also suffer from hyperuricemia due to increased cell death and conversion of adenosine monophosphate to uric acid.[61] If uric acid levels are not reduced after an acute gout flare, reoccurrence is much more likely, with 75% of patients suffering from gout reoccurrence within a 2-year period.[65] Chronic gout develops when the accumulation of larger urate tophi, or deposits of urate crystals, accumulate in the joints and surrounding tissue, leading to recurrent, more intense, gout flares.[70]

A brief overview of purine metabolism is useful in understanding how uric acid accumulates in the joints. In the human body, purines are processed via a long sequence of complex enzymatic reactions that begins with adenine and guanine, the two purine nucleic acids, and ends with uric acid.[62] Xanthine oxidase, plays a critical role in the production of this compound, as it catalyzes the oxidation of xanthine to uric acid, producing hydrogen peroxide during the process.[62] Uric acid is then excreted through the urinal or gastrointestinal tract, preventing uric acid accumulation in the body. Hence, dysfunction of the kidneys is a major risk factor for gout. Therefore, therapeutic approaches to reducing uric acid production through xanthine oxidase inhibitors, such as allopurinol and febuxostat, are the primary method used to treat hyperuricemia in gout patients.[71]

2.3 Current Methods of Uric Acid Measurement

Treating and managing gout requires maintaining low uric acid concentrations for extended periods. In fact, patients who have been diagnosed with gout are often advised to maintain serum urate concentration below 6 mg/dL for several years to allow for the dissolution of urate crytals.[72] Failure to manage gout can lead to a progression of the disease from an acute phase to a chronic tophaceous phase. During this phase, which is much harder to treat, uric acid crystals accumulate in the synovial spaces in greater volumes.[68,70]

Maintaining low serum urate concentrations requires frequent measurements, along with diet adjustments and the use of anti-hyperuricemic medication. However, current methods of uric acid measurement present a barrier for many patients. In fact, even after gout diagnosis, studies show that only 20% of patients obtained measurements of serum uric acid concentration, despite the failure of 40 – 80% of them to achieve target uric acid concentrations of below 6 mg/dL.[73]

The low compliance to uric acid measurement is likely due to the cost and inconvenience of the current clinical standard methods of uric acid measurement. These techniques primarily consist of laboratory tests where high performance liquid chromatography (HPLC), colorimetry, and electrochemical techniques are performed on blood and urine samples obtained from patients.[74-77] Due to the required materials and labor, such techniques can be slow, costly, and are not practical for frequent monitoring of uric acid in chronic gout patients. Hence, the use of affordable, easy-to-use biosensors for uric acid measurements presents a compelling alternative to current standards.[69]

The physiological concentration of uric acid typically ranges from 1.5 to 7.0 mg/dL in healthy patients and 7.4 to 8.7 mg/dL in hyperuricemic patients.[62,78] Hence, uric acid biosensors should be capable of resolving uric acid changes around a 0 – 10 mg/dL analyte range. As explained earlier, hyperuricemia is the primary concern in gout. Therefore, monitoring hypouricemia, which occurs when uric acid levels fall below 2 mg/dL, is not nearly as critical as in glucose biosensors, where a failure to detect low analyte concentrations can be fatal. Other design considerations for uric acid biosensors include achieving high reproducibility and sensitivity, which can vary widely depending on the method of uric acid detection and signal transduction, with electrochemical biosensors generally being more sensitive than optical biosensors.[79-81]

2.4 Enzymatic Electrochemical Uric Acid Biosensors

To create a more patient-friendly means of uric acid measurement, researchers worldwide have explored the development of affordable, point-of-care uric acid biosensors using a wide range of approaches.[77,82-87] The most prevalent type of these biosensors operate through electrochemistry and can be divided into two categories, non-enzymatic and enzymatic.[88] Non-enzymatic

electrochemical uric acid biosensors operate by exploiting the electroactive nature of uric acid by using electrodes to oxidize uric acid into allantoin, CO_2 and H_2O_2.[69] However, such techniques are susceptible to interference from alternate electroactive species like ascorbic acid.[88]

Most uric acid biosensors in research are of the enzymatic electrochemical nature.[69] With the use of uric acid oxidase, or uricase, as a biorecognition element; enzymatic electrochemical biosensors generally show greater sensitivities than their non-enzymatic counterparts. However, many electrochemical enzymatic biosensors still suffer from selectivity issues due to the use of electrodes and peroxidases.[89] Specifically, this class of biosensors work by generating H_2O_2 ensuing the catalysis of uric acid by uricase. H_2O_2 is then measured by a peroxidase or electrode to indirectly determine uric acid concentration. The presence of electroactive species in human serum can therefore interfere with uric acid measurements. Hence, despite considerable research progress in this domain, the translation of electrochemical uric acid biosensors from research projects into commercial products have been slow, and very few of these devices have obtained FDA approval.[69]

2.5 Optical Uric Acid Biosensors

Though not as common electrochemical methods, a variety of optical biosensors have been explored for the detection of uric acid. Several of these techniques are based on the use of absorbance,[90] fluorescence,[82,85,91] and surface plasmon resonance.[92,93] There are a few key advantages of optical biosensing over electrochemical methods. Firstly, they eliminate the need for electrodes and peroxidases that can otherwise be affected by alternate electroactive interferents, such as glucose, urea, and ascorbic acid. The use of optically responsive probes, such as fluorophores, phosphors, metallic nanoparticles, and chromogenic agents; although not without their challenges, mitigate the interference issue.

Secondly, optical probes are excellent tools for the design and fabrication of implantable biosensors that eliminate the painful process of drawing blood samples. For instance, optical biosensing allows for the possibility of transdermal interrogation of miniature biocompatible hydrogel implants by an optical transmitter situated on the surface skin. Developing fully implantable electrochemical biosensors is currently not as feasible, due to the difficulty of miniaturizing the required electronics and the inability to physically decouple the bioreceptor, signal transducer, and signal processor, which require a power source to function. An implantable uric acid biosensor would be especially well suited for geriatric patients, who suffer from chronic gout and suffer from limited joint mobility and dexterity needed to perform finger pricks. With an implantable uric acid biosensor that passively monitors and records *in vivo* uric acid fluctuations, these patients will be better able to keep their levels under the threshold needed to dissolve uric acid tophi, and avoid the occurrence gout attacks, while understanding how their diet and lifestyle habits influence their uric acid levels.

2.6 Porphyrin-Oxidoreductase Biosensing Platform

Most current optical biosensing techniques for uric acid detection are not well suited for implantation applications due to optical signal interference from autofluorescence and light scattering from surrounding tissue.[94] Long-lifetime phosphorescent probes for signal transduction can used to solve this challenge. McShane and coworkers have demonstrated the use of metalloporphyrin probes, with phosphorescence lifetimes that are hundreds of microseconds long, in the development of implantable biosensors capable of detecting glucose, lactate, and oxygen.[51-53] These sensors are fabricated by coimmobilizing, oxygen-sensitive metalloporphyrin molecules (signal transducers) and oxidoreductase enzymes (bioreceptors) within a hydrogel matrix.

This porphyrin-oxidoreductase platform is the basis of this study, which describes the fabrication and characterization of the first implantable uric acid biosensor based on phosphorescence. In this system, the consumption of oxygen during the catalysis of the oxidation of uric acid into allantoin, carbon dioxide, and hydrogen peroxide by uric acid oxidase leads to a local depletion of oxygen as shown in the following reaction and in Figure 2-2.

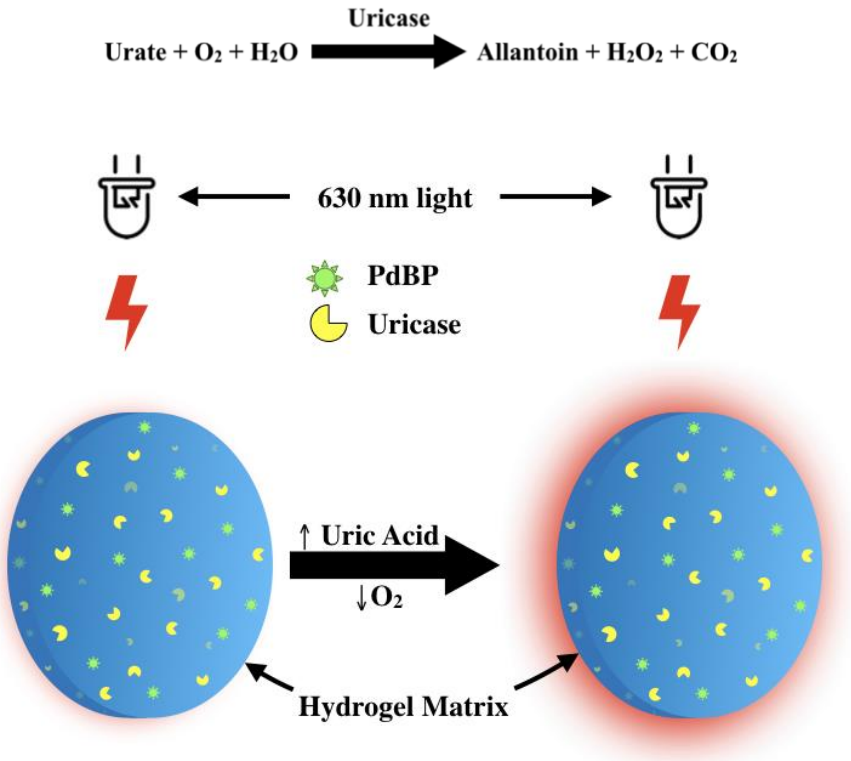

Figure 2-2: A schematic of the excitation of a uric acid biosensor, containing BMAP and uric acid oxidase

These local oxygen changes within the biosensor matrix leads to a measurable alteration of an optical signal. Specifically, a decrease in oxygen concentration leads to an increase in phosphorescence intensity and lifetime due to the collisional quenching of the excited phosphor by oxygen. Intensity and lifetime are therefore proportional to analyte concentration and inversely proportional to local oxygen concentration.

Phosphorescence lifetime, as opposed to luminescent intensity, was used for the transcutaneous optical signal transduction due to the temporal separation of the signal from background noise and autofluorescence. The collisional quenching of palladium (II) tetramethacrylated benzoporphyrin (BMAP) in generally described by the Stern-Volmer relationship:

$$\frac{I_0}{I} = \frac{\tau_0}{\tau} = 1 + K_{sv}[O_2]$$

Where I and τ represent the luminescence intensity and lifetime at a specific concentration of oxygen, while I_0 and τ_0 represent the intensity and lifetime in the absence of oxygen. The Stern-Volmer constant (K_{sv}), characterizes the oxygen sensitivity and is the slope of the Stern-Volmer graph. Therefore, the intensity and phosphorescence lifetime are inversely proportional to the oxygen concentration and directly proportional to the concentration of uric acid. Besides the long phosphorescence lifetime, another key advantage of using BMAP in implantable biosensor applications is the long excitation wavelength of the phosphor. This allows for excitation in the "optical therapeutic window," where absorption from water and proteins are low (detailed in section 4.3).

Overall, the function of the porphyrin-oxidoreductase biosensing platform is a complex balance of uric acid diffusion, enzymatic reaction rate, and oxygen diffusion. In this uric acid biosensing system, the performance of the uric acid biosensor was regulated by tuning the swelling of the biosensor matrix (detailed in section 4.2) in order to adjust the diffusion of uric acid into the hydrogel and the sensitivity of the biosensor. The strategy, rationale, and test results for the selection of these materials are further explained the following sections.

3. MATERIALS AND METHODS

This section describes the design, fabrication, and evaluation of enzymatic optical uric acid biosensors for implantable and *ex-vivo* applications based on the use of uricase a biorecognition element, and porphyrin molecules for optical signal transduction. Specifically, uricase and BMAP were immobilized in three copolymers of 2-hydroxyethyl methacrylate (HEMA) and acrylamide (AAm). In addition to a description of the rationale, design, and characterization of the uric acid biosensor system, the effect of copolymer composition on the swelling ratio, oxygen response, and uric acid response was determined. Relevant metrics, such as the sensitivity, limit of detection, selectivity, and storage stability are also detailed.

3.1 Materials

2,2-dimethoxy-2-phenyl-acetophenone (DMAP/Irgacure 651) and ethylene glycol were obtained from Sigma (St. Louis, MO, USA). 2-Hydroxyethyl methacrylate (HEMA), Ophthalmic Grade, and triethylene glycol dimethacrylate (TEGDMA), min 95% were purchased from Polysciences, Inc (Warrington, PA). Acrylamide (AAm) monomer and dimethyl sulfoxide (DMSO) were acquired from VWR (Radnor, PA, USA). Palladium (II) tetramethacrylated benzoporphyrin (BMAP or PdBP) was donated by Profusa, Inc. (San Francisco, CA). Uric acid was purchased from USB Corporation (Cleveland, OH), while uric acid oxidase/uricase from recombinant Escherichia coli (E. coli) was acquired from BBI Solutions (Cardiff, UK).

3.2 *In-vitro* Testing System and Instrumentation

A benchtop testing system, consisting of a newly-designed Delrin flow cell (detailed in section 4.1), a previously-designed optics system, along with commercially-available peristaltic pumps and incubators were used to conduct oxygen and uric acid response tests. Optical readers

for sample interrogation were mounted onto the Delrin flow cell, which contained four biosensor samples (three experimental samples, and one enzyme-free reference). Each reader contained a red LUXEON Rebel LED from Lumileds (Amsterdam, Netherlands), powered at a current of 200 mA, and was used to excite samples around 630 nm. Readers also housed photomultiplier tubes (SensL, Cork, IR), positioned 8 mm away from the LED, and used to collect the emission signal after collimation by an emission filter (FF02-809/81, Semrock).

Buffer solutions containing select uric acid and oxygen concentrations were supplied to the flow cell using a Masterflex L/S Series peristaltic pump purchased from Cole-Parmer (Ct Vernon Hills, IL). Oxygen and uric acid testing systems shared a similar equipment setup. The primary differences between both were the type of solutions used, and the choice of a closed loop design for oxygen response tests versus a flow-through design for uric acid response tests, the specific set-ups are detailed in Sections 2.6 and 2.7.

A LabVIEW program was used to control the LED in the optical reader during the excitation and emission phase. For emission, an excitation pulse from the LED was generated for 500 µs. Following excitation, the LED was switched off for 2500 µs while the voltage across the PMT was measured and used to calculate the phosphorescence emission lifetime (τ). A brief waiting period of 7 µs between excitation and emission was granted to reduced interference. An Infinite 200 PRO 96-well plate reader (Tecan Life Sciences, Switzerland) was used to conduct absorbance and emission scans. Free radical polymerization was performed using a Blak-Ray B-100SP UV Lamp purchased from UVP (Upland, CA).

3.3 Selection of Hydrogel Compositions

The hydrogel matrix plays a central role in the structure and function of the biosensing system. Not only does it immobilize the enzyme and dye, but regulates the diffusion of uric acid

into the matrix, which influences biosensor response. Hence, careful selection of a hydrogel material that provides tunable diffusion properties, biocompatibility, and a suitable chemical environment for homogeneous dispersion of the immobilized sensing chemistry is key to developing an effective uric acid biosensor. To serve this purpose, a copolymer system of 2-Hydroxyethyl Methacrylate (HEMA) and acrylamide (AAm) was used (Figure 3-1).

HEMA hydrogels have been extensively studied, and are used in a variety of biomedical applications, from controlled drug release to soft contact lenses fabrication.[95] This material was selected as the primary monomer for the uric biosensor matrix due to its chemical stability, strong mechanical properties, high optical clarity, and biocompatibility.[96] Despite these desirable properties, the swelling ratio of HEMA is thermodynamically restricted to just 40%.[97] As a result, HEMA is frequently copolymerized with more hydrophilic monomers, like methacrylate and acrylamide (AAm).[97,98] Most known for its use in gel electrophoresis, AAm is a highly absorbent material that possesses good optical properties and biocompatibility, ideal for the use in a biosensor.[96] Therefore, adjusting the ratio of AAm added to the copolymer provides a means of tuning the swelling of the biosensor hydrogel matrix, while retaining optical clarity, mechanical integrity, and biocompatibility.[51,52]

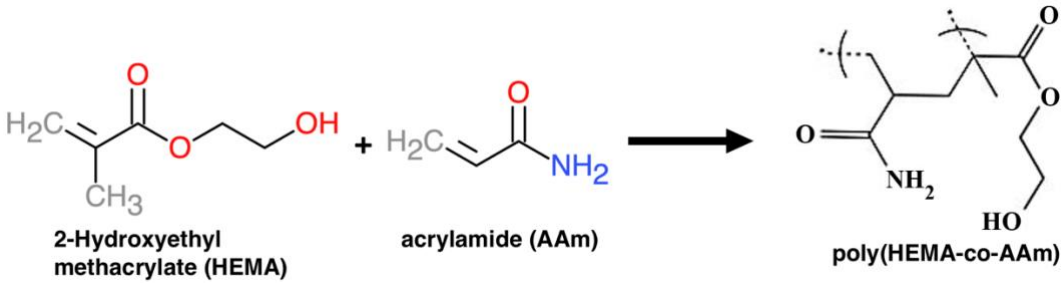

Figure 3-1: Chemical Structure of acrylamide (AAm), 2-hydroxytheyl methacrylate (HEMA), and poly(HEMA-co-AAm) (adapted from Rapado and Peniche, 2015)[97]

Modification of the swelling ratio of the hydrogel matrix allows for regulation of uric acid diffusion into the biosensor. Less-swollen hydrogels create a more tortuous path for uric acid

diffusion towards immobilized uricase enzymes, which leads to reduced oxygen depletion and as a result, lower phosphorescence lifetimes and biosensor sensitivity. Specifically, assuming the catalysis of uric acid oxidation is analyte-limited, versus oxygen or enzyme limited (explained in greater detail in Section 4.5), the rate of uric acid diffusion into the hydrogel matrix dictates the amount of oxygen depletion by uric acid oxidase and therefore the magnitude of optical response of the biosensor.

This phenomenon was observed in prior glucose diffusion studies conducted by our group, where a 30-fold increase in analyte diffusivity was observed in a copolymer of HEMA and AAm (50:50 molar ratio) versus a polyHEMA homopolymer. This increase in diffusivity translated to a 6-fold increase in biosensor sensitivity.[99] We therefore hypothesize that the uric acid biosensor sensitivity can be improved by increasing the concentration of acrylamide. To test this hypothesis, three hydrogel compositions of poly(HEMA-co-AAm) were fabricated with molar ratio 50:50, 75:25, and 90:10 molar ratios of HEMA and AAm respectively. Prior studies showed increased sample variation and decreased repeatability in hydrogel compositions with AAm ratios greater than 50% due to phase separation. Therefore, the 50:50 composition was set as the upper limit for acrylamide concentration.[52,99]

3.4 Biosensor Fabrication

Hydrogels were fabricated using free-radical polymerization of monomer precursor solutions, crosslinker, copolymer solutions, enzyme mixture, and dye solutions. The difference in the fabrication procedure between each copolymer composition was in the volume of HEMA or AAm monomer added. HEMA was available in liquid form, while an AAm solution was made by dissolving crystalline powdered AAm monomer in deionized water to form a 0.67 w/v%. Appropriate volumes of each monomer solution was added to collectively produce a 250 µL

solution (i.e. 125 µL of HEMA solution was combined with 125 µL of the AAm solution to create a 50:50 poly(HEMA-co-AAm) precursor composition).

The detailed gel fabrication steps are as follows: (1) 2.5 mg Igracure 651 was weighted into a 2.5 ml microcentrifuge tube, (2) pre-calculated volumes of HEMA and AAm monomer solution were addedbefore vortexing, (3) 5 µL of TEGDMA (crosslinker) was pipetted into the monomer mixture, (3) 90 µL of ethylene glycol (co-solvent) was added to the mixture, which was vortexed again, (4) 12.5 µL of a 10 mM BMAP solution dissolved in DMSO was pipetted to the centrifuge tube, and (5) 49 mg (125 units) of uricase, along with 107.5 µL of PBS (pH 7.4) was added to the solution. Prior to gel fabrication, a "sandwich" glass mold was made using paperclips to clamp a 0.03'' Teflon spacer between two glass slides.

The mixture was repeatedly pipetted for a few minutes to improve the homogeneity of the sensing chemistry in the precursor solution before being pipetted into the premade glass mold. The precursor-loaded mold was placed under a UV lamp, emitting light of 365 nm, for photopolymerization of the precursor solution for 3 minutes on each side. After crosslinking, the gel slab is carefully removed from the mold, rinsed with DI water and placed in a 45 ml tube centrifuge tube containing PBS (pH 7.4) and allowed to equilibrate overnight in a 4 ºC refrigerator. Afterwards, gels were rinsed with DI water, placed in fresh PBS, and again stored in 4 ºC. During storage, tubes containing gels were wrapped in aluminum foil to avoid photobleaching of the immobilized phosphor. For later experiments, thin disc-shaped samples were punched from fabricated hydrogel slabs using a 6 mm biopsy punch (VWR, PA).

3.5 Swelling Ratio

To calculate the swelling ratio, 3 freshly-made samples of each composition were weighed for their hydrated mass W_s after soaking overnight in PBS (pH 7.4) to reach their equilibrium

swelling volume. Prior to this step, samples were blotted to remove excess buffer on the surface of hydrogel discs. Next, samples were desiccated for 24 hours and then weighed for their dry mass W_s. The final swelling ratio was obtained using the following equation:

$$Swelling\ Ratio\ = \frac{W_s - W_d}{W_d} \times\ 100$$

3.6 Oxygen Response

An understanding of how the phosphorescence lifetime of the uric acid biosensors vary with oxygen concentration is critical to understanding biosensor function. Doing so characterizes the biosensor sensitivity to oxygen and defines the absolute achievable lifetime range of the immobilized phosphors within a hydrogel matrix. Therefore, before introducing uric acid, the response of biosensors of each composition to changes in oxygen was assessed.

After gel fabrication, 6 mm punches were made from the larger hydrogel slab and placed in the flow cell for monitoring. The flow cell was then connected to the *in-vitro* testing system described in Section 3.2. Each flow cell contained 3 replicate samples and 1 non-uricase containing oxygen sensor reference gel. Biosensor responses to oxygen changes were tested by exposing the gel samples to 10 mM PBS buffer (pH 7.4) with oxygen concentrations ranging from 0 – 206.8 µM. Oxygen response tests were conducted in the following sequence: 206.8 µM (21 %), 103.4 µM (10.5 %), 51.7µM (5.25 %), 25.9µM (2.6 %), and 0 µM oxygen. These oxygen concentrations, which encompass low physiological concentrations through ambient oxygen concentrations, were controlled using a mass flow controller to bubble in controlled ratios of nitrogen and ambient air into a sealed reservoir containing the PBS in a closed-loop system (Figure 3-2). The final 0 µM oxygen concentration was achieved chemically through due to limitations in removing all oxygen using the gas bubbling method. To purge all dissolved oxygen from the flow cell, a 1 M solution of glucose dissolved in PBS buffer was combined with a 6 mg/dL solution of glucose oxidase

dissolved in DI water solution. Solution were added in a 4:1 ratio to completely fill the flow cell, with special care taken to avoid air bubbles forming in the flow cell. For each oxygen concentration, data were collected for at least 30 minutes after a steady state response was achieved.

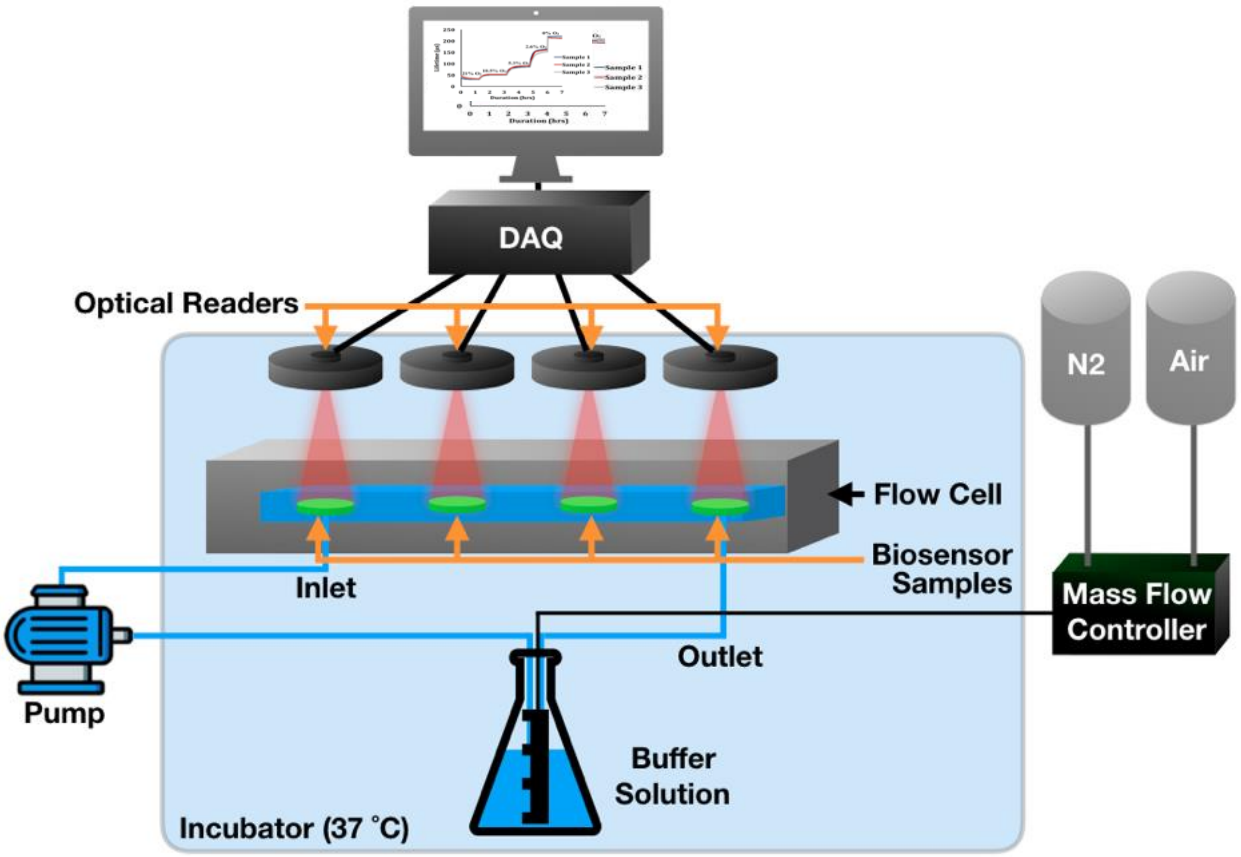

Figure 3-2: *In vitro* oxygen testing system

3.7 Uric Acid Response

Figure 3.3 illustrates the benchtop setup for uric acid response testing, which strongly resembles the previously described oxygen test setup with a few differences. Namely, pre-made uric acid solutions were used instead of plain PBS buffer. Uric acid solutions consisted of uric acid dissolved in 10 mM PBS buffer (pH 7.4). A range of 0 – 10 mg/dL of uric acid was tested in serial increments of 2 mg/dL. As with the oxygen response tests, data were collected for at least 30

minutes after steady state was achieved, with each step taking a total of 45 – 60 minutes. The other notable difference between this system and the oxygen response testing system was in the unidirectional flow-through approach. Here, the solution from the outlet was not reused but collected in a large waste container.

After data collection, the phosphorescence lifetime as a function of uric acid concentration was plotted. The sensitivity was calculated as the slope of this line, while the limit of detection was estimated as the uric acid concentration corresponding to the phosphorescence lifetime at 0 mg/dL plus 3 times the standard deviation at 0 mg/dL. After comparing these biosensor metrics, the hydrogel composition with the lowest limit of detection and greatest sensitivity was chosen for all ensuing experiments.

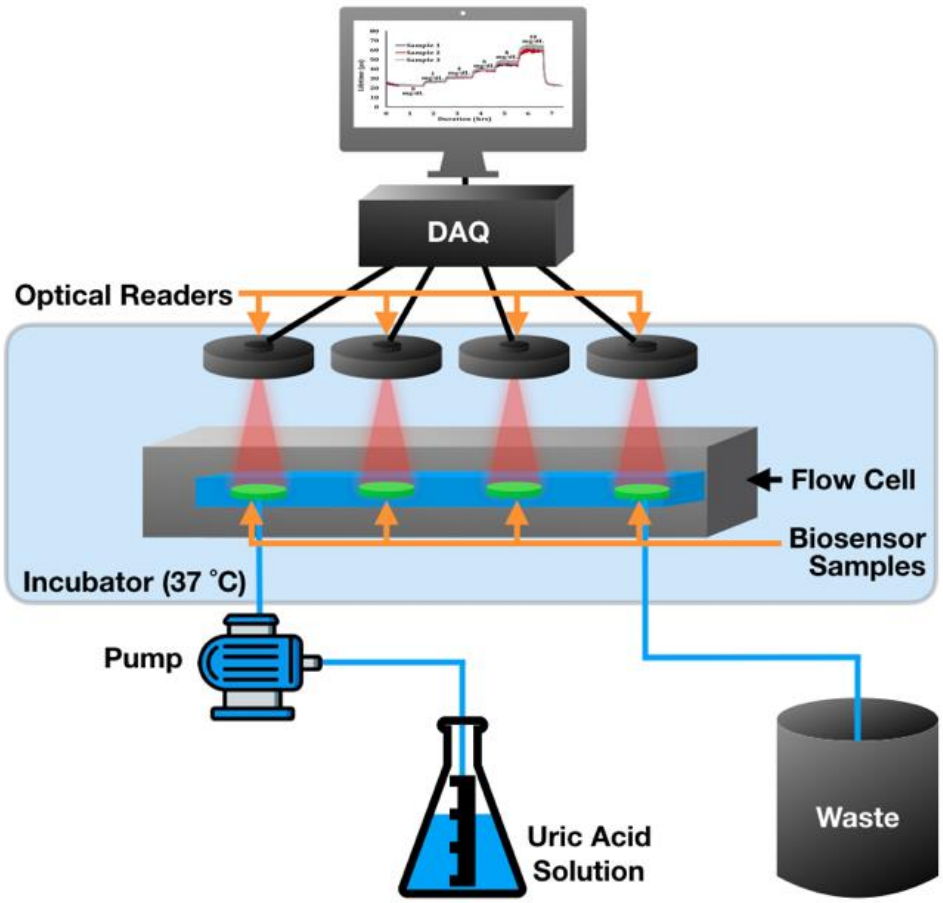

Figure 3-3: *In vitro* uric acid testing system

3.8 Selectivity

To assess the selectivity of system, biosensor responses to several alternate analytes present in human serum were evaluated and compared to the response to uric acid. These analytes included glucose, ascorbic acid, urea, allantoin, creatinine, and acetaminophen. Solutions of physiological concentration of each analyte were made using PBS buffer (pH 7.4). Using the flow-through system, each solution was individually exposed to the uric acid biosensor samples for an hour each after a 1-hr "warm-up" period, where plain buffer was used to obtain a baseline response for each sample. Percent changes of the phosphorescence lifetimes for each analyte from the baseline response was calculated and reported.

3.9 Storage Stability

To characterize biosensor stability, two types of stability tests were performed: cyclic tests and storage tests. Cyclic stability tests were performed by sequentially exposing uric acid biosensors to solutions of 0 and 10 mg/dL uric acid for an hour each, using the previously described flow-through system to run a total of 20 cycles. These concentrations of urate represent the minimum and maximum concentration of urate within our analytical range. Afterwards, the percent change in sensor response between cycles was calculated.

The storage stability of the uric acid biosensors was also assessed to evaluate the long-term viability of the sensors from possible loss of enzyme bioactivity. Specifically, uric acid-bioresponsive slabs were stored in two conditions. Storage condition 1 was in 45 ml of PBS with no uric acid, while storage condition 2 was in 45 ml of a 6.8 mg/dL uric acid solution. Both solutions were kept at 23 °C at pH 7.4. To partially address the inevitable change in uric acid concentration in condition 2, the uric acid solution was replaced weekly. Disc samples were punched and tested using the flow-through system after 0, 4, and 8 weeks of storage.

4. RESULTS AND DISCUSSION

4.1 Flow Cell Fabrication

Using SolidWorks, two identical flow cells were designed for *in-vitro* assessments of biosensor samples. The following considerations were made when selecting the material for the flow cell: mechanical strength, chemically inertness, durability, thermal expansion and light reflectance. Delrin, or polyoxymethylene, is a widely used, mechanically robust, thermoplastic material that largely fulfils these criteria. Not only is Delrin relatively easy to machine, but it possesses a metal-like high yield strength and wear resistance, despite being a thermoplastic material.[100] Although susceptible to alkaline oxidation, Delrin is resistant to corrosion from most solvents and since the flow cell was to be used with mild buffered solutions around a neutral pH, corrosion was not a concern.

For the simultaneous testing of 3 experimental samples and 1 oxygen reference, the flow cells were designed to hold 4 samples (Figure 4-1). Each flow cell consisted of a top half (Figure 4-2), with hollow indents to secure the optical readers during testing, and a bottom half with a narrow channel to allow fluid flow (Figure 4-3). On the bottom plane of the bottom half, threaded holes were made to allow for easy connection to tubes connecting the flow cell to peristaltic pumps and fluid reservoirs. The 3-D model for the top and bottom halves were designed in SolidWorks and professionally machined using a CNC mill.

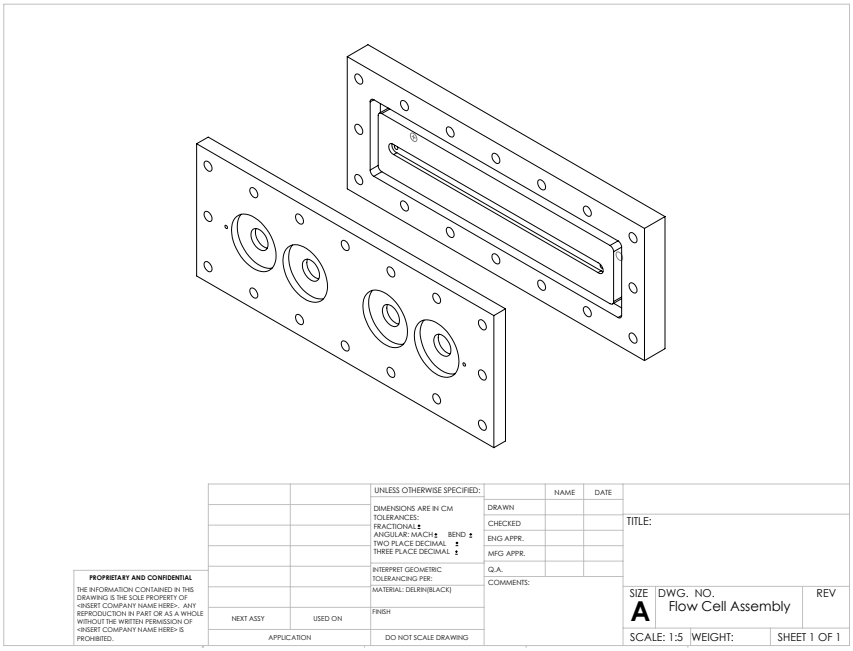

Figure 4-1: Isometric view of the top and bottom halves of the Delrin flow cell

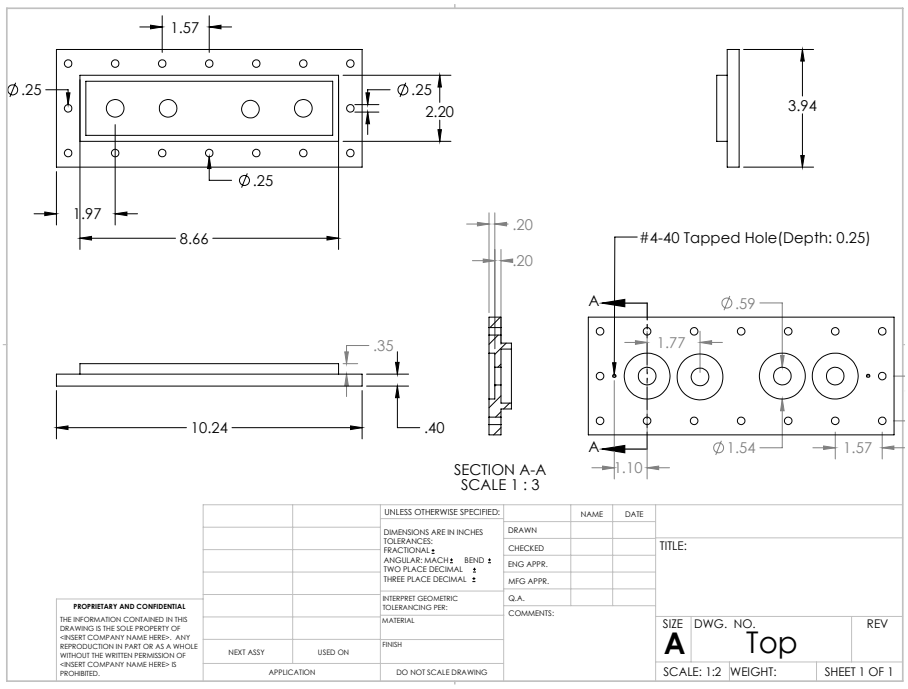

Figure 4-2: Engineering drawing of the top half of the Delrin flow cell

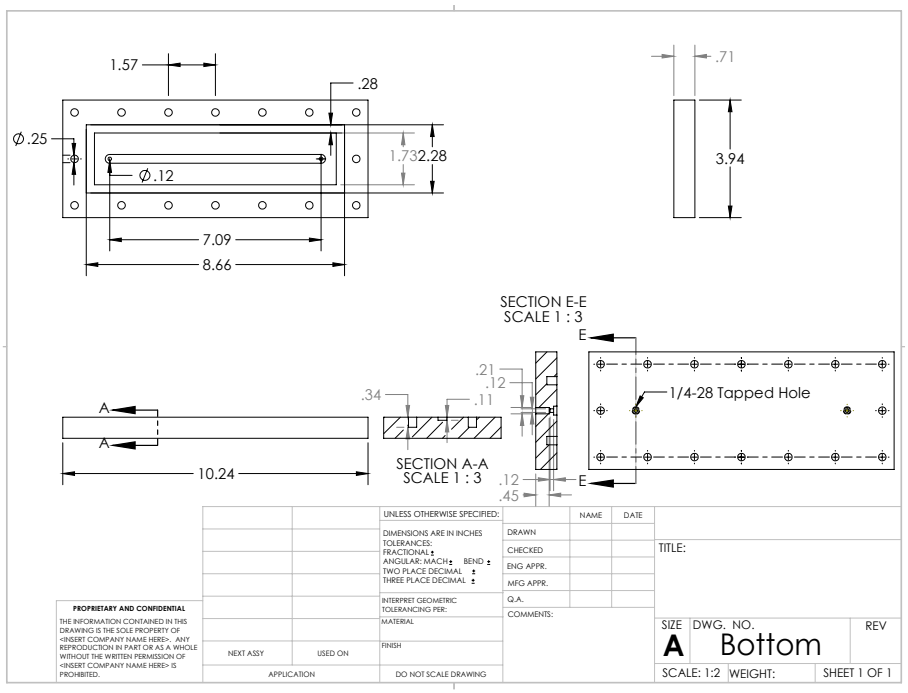

Figure 4-3: Engineering drawing of the bottom half of the Delrin flow cell

Between both halves of the flow cells, a laser-cut, transparent acrylic rectangle piece (1” x 8” x 0.1”) was used to mount the hydrogel samples (Figure 4-4). Miniature, half torus-shaped black silicone “scorpion tails” were used to clamp down the hydrogel samples in place to withstand flow. Finally, thin black silicone sheets were used to create a water-tight seal between the two halves of the flow cells, which were securely screwed together to prevent leakage.

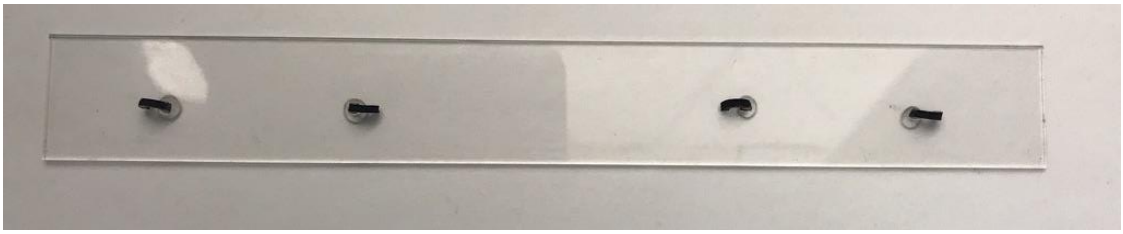

Figure 4-4: Acrylic slide with black silicone sample clamps

4.2 Swelling Ratio

Due to differences in molecular structure, HEMA and AAm possess very different levels of hydrophilicity, and therefore different swelling ratios. Although generally considered

hydrophilic, polyHEMA is much more hydrophobic than polyacrylamide. This likely primarily due to two reasons. Firstly, the presence of hydrogen bonds between hydroxyl group of polyHEMA likely inhibits the swelling of material.[101] Similar intra- and intermolecular hydrogen bonding between hydroxyl groups of HEMA and amine side chains of AAm[102] have been identified in literature, using Fourier-transform infrared spectroscopy (FTIR),[97] when HEMA is copolymerized with AAM. Secondly, the non-polar methyl group present in the primary structure of HEMA likely reduces the hydrophilicity of the material, despite the polarity of the hydroxyl groups. In contrast, no pendant methyl groups exist in the primary structure of AAm to reduce the hydrophilicity created by polar amine groups in the compound.

Therefore, increasing the concentration of acrylamide should increase the swelling ratio of uric acid biosensors with poly(HEMA-co-AAm) hydrogel matrices. As shown in Table. 4-1, testing the swelling ratio of the three copolymers compositions (50:50, 75:25, and 90:10 poly(HEMA-co-AAm) yielded results that supported this hypothesis.

Table 4-1: Swelling Ratios of Uric Acid Biosensors

Hydrogel Composition	Swelling Ratio
50:50 poly(HEMA-co-AAm)	249 ± 9.81
75:25 poly(HEMA-co-AAm)	131 ± 4.32
90:10 poly(HEMA-co-AAm)	100 ± 6.19

When compared to the 90:10, composition, the 75:25 composition had a 30% increase in swelling ratio, while the 50:50 composition had a massive 250% increase in swelling ratio. This difference in magnitude of acrylamide-dependent hydrogel swelling seen in the three hydrogel compositions implies that the relationship between swelling ratio and acrylamide concentration is more exponential than linear. Hydrogel swelling is primarily dependent on the molecular structure of the polymer network, and a closer look at the chemistry of acrylamide reveals an interesting

insight to the disproportionate increase in swelling. Specifically, in a pHs above 6, acrylamide moieties are believed to be partially hydrolyzed, forming negatively-charged carboxylate ions.[103,104] Since all hydrogel samples were tested and stored in PBS buffers around a pH of 7.4, this alkaline hydrolysis of acrylamide-rich gels may have further drove hydrogel swelling due to electrostatic repulsion by carboxylate ions.

4.3 Absorbance and Emission Spectra of Uric Acid Biosensors

Conducting transdermal interrogations is often a difficult challenge in the development of optical biosensors, due to autofluorescence and optical interference from the surrounding tissue. Near IR, phosphorescent, metalloporphyrin probes present a possible solution to this issue, due to their ability to operate within the "optical therapeutic window," which occurs around 650–950 nm. In this range, autofluorescence, scattering, and absorption of light by pigments, such as hemoglobin, that occurs in shorter wavelengths is minimal. Additionally, light absorbance by water, which is prevalent at longer wavelengths, can also be avoided.[105] Other advantages of metalloporphyrin probes for use as optical transducers are their large Stokes shifts, high quantum yields, and extremely long phosphorescence lifetimes granted by triplet excited states.[106]

Besides their photophysical properties, another key feature of near IR metalloporphyrin probes lies in their inherent responsiveness to changes in oxygen concentration. In the presence of oxygen, the luminescent intensity and phosphorescence lifetimes of these molecules are collisionally quenched due to the non-radiative energy transfer between the excited phosphor to molecular oxygen.[107] Oxygen-sensitive metalloporphyrin probes for *in vivo* monitoring were first synthesized in 1995 by Vinogradov and Wilson [108] in the form of tetrabenzoporphyrins. The quantum yield and photostability of these molecules were improved by Niedermair et al.,[109] as a

result, the viability of benzoporphyrins as optical probes of implantable biosensors has become much more viable.

The excitation and emission spectra of Palladium (II) tetramethacrylated benzoporphyrin (BMAP), the benzoporphyrin molecule used in this study, was obtained and displayed in Figure 4-5 (A) and (B). An absorption and emission peak of BMAP (Figure 4-6) occurred around 633 and 795 nm respectively. This finding indicates that optical transduction of the uric acid biosensor occurs in the near-IR region, which would enable for transdermal interrogation of biosensor implants with minimal optical scattering, autofluorescence, and absorption. Although, the peak excitation wavelength falls before the optical window, the excitation signal still falls in the red wavelength range and should therefore be sufficient for sample interrogation.[105]

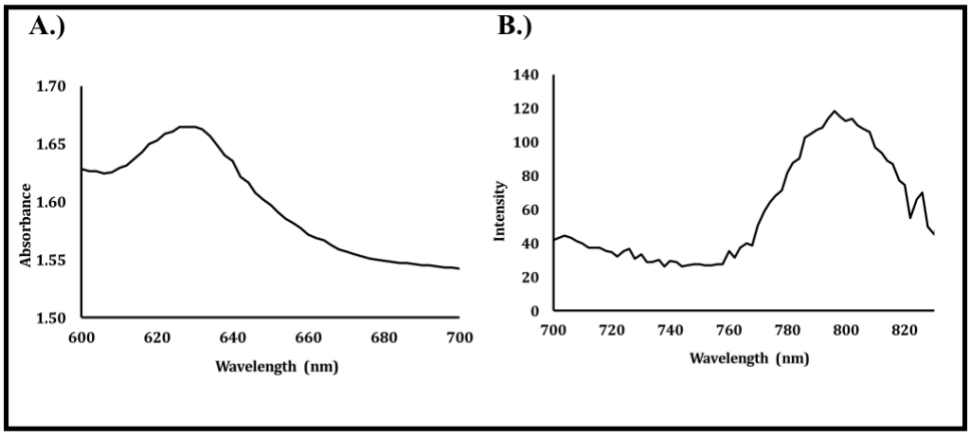

Figure 4-5: (A) Excitation and (B) emission spectra of BMAP in 50:50 poly(HEMA-co-AAm)

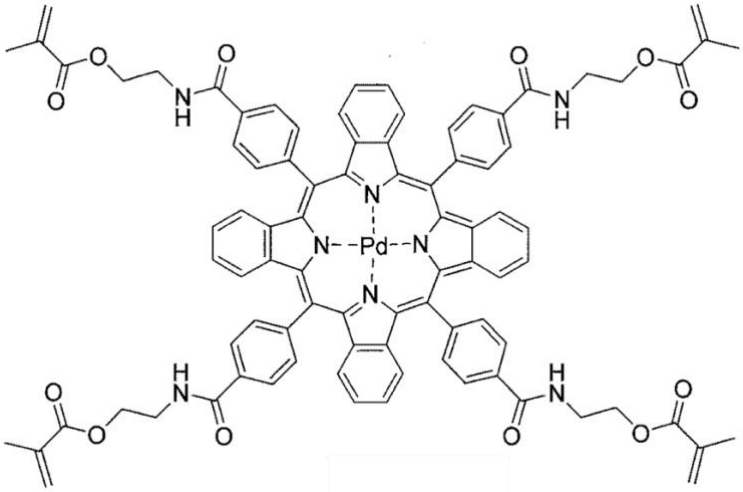

Figure 4-6: Chemical structure of Palladium (II) tetramethacrylated benzoporphyrin (BMAP)

4.4 Effect of Oxygen Concentration on Phosphorescence Lifetime

When oxygen-sensitive phosphors are closely coupled with oxidoreductase enzymes and immobilized in a hydrogel matrix, capable of absorbing analyte-rich solutions, an optical biosensor is created. The combination of these three elements are the essence of the described system: BMAP as the oxygen-sensitive phosphor, uricase as the oxidoreductase enzyme, and poly(HEMA-co-AAm) as the biocompatible hydrogel matrix.

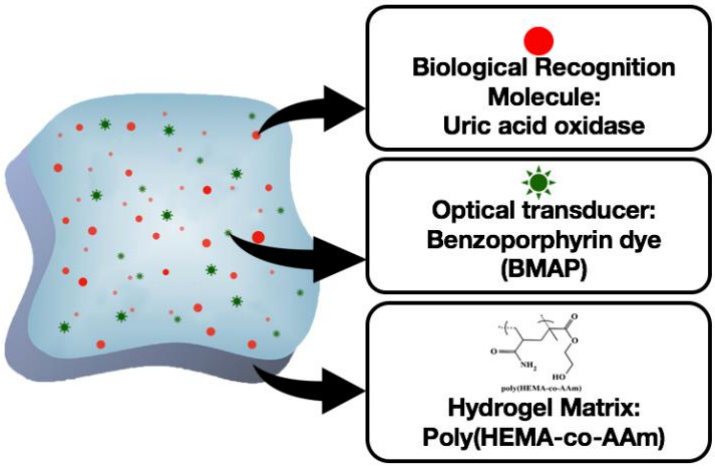

Figure 4-7: An illustration of the contents of the uric acid-responsive hydrogel

Together, they produce an optically responsive hydrogel. In the presence of uric acid, uricase drives the local depletion of oxygen and leads to a detectable increase in phosphorescence lifetime of BMAP. Central to the function of this system is the phenomenon of collisional quenching. This occurs due to the non-radiative transfer of energy between BMAP, at an excited energy state, to oxygen, of concentration $[O_2]$, and is described by the Stern-Volmer relationship provided in Section 2.6. Figure 4-8 (B) shows the Stern-Volmer plot, which the is normalized phosphorescence lifetime of all three hydrogel compositions as a function of oxygen concentration. Stern-Volmer quenching constant (K_{sv}) is the slope of the Stern-Volmer plot , and can be used to quantify oxygen sensitivity of each hydrogel composition.

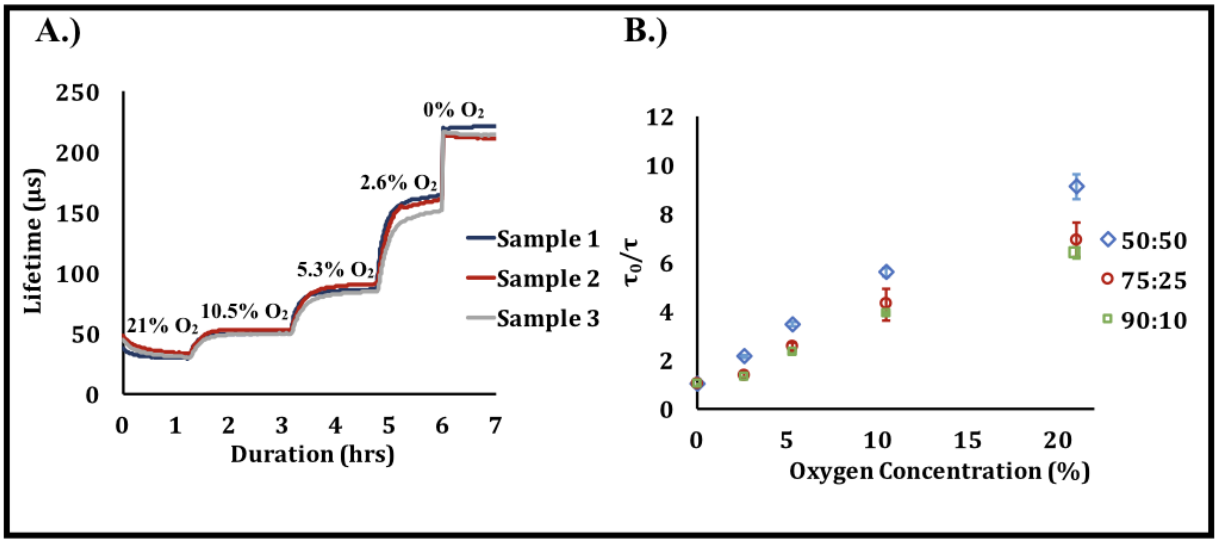

Figure 4-8: Effect of oxygen on phosphorescence lifetime. (A) Representative raw data (B) Stern-Volmer plot of all hydrogel compositions

As shown in **Table 4-2**, the K_{sv} values were not significantly different among the three compositions, despite their slight increase in compositions with greater concentrations of acrylamide. This finding is in accordance with our expectations derived from prior studies, that imply that K_{sv} values should be approximately identical all compositions, since molecular oxygen is miniscule in size when compared to uric acid and the hydrogel mesh.[52]

Another major factor that influences the K_{sv} values is the complex chemical environment of hydrogel matrix. The hydrogel chemical environment affects the interaction between the sensing chemistry and PBS; as well as the dispersion of BMAP within the hydrogel matrix. Despite not being significant, there is an observed increase in K_{sv} values of compositions with greater concentrations of acrylamide (Table 4-2), which implies that greater oxygen quenching occurred in these compositions, perhaps due to the increased hydrophilicity providing greater access of the immobilized phosphors to molecular oxygen in the absorbed buffer. Since all measurements were conducted after steady state was achieved (i.e. a flat response was observed on the oxygen response curves), it is unlikely that the greater swelling ratios, seen in copolymers with greater acrylamide concentrations, is directly responsible for the higher oxygen sensitivity. In other words, after steady-state, we can assume that oxygen concentrations in all gels are approximately equal. What dictates the oxygen sensitivity of each hydrogel composition is the interaction, or lack thereof, between the phosphors and the local aqueous environment, and not the oxygen diffusion rate into the hydrogel matrix.

Table 4-2: Stern-Volmer Constants of Uric Acid Biosensors

Composition	K_{sv} (% O_2)$^{-1}$
50:50 poly(HEMA-co-AAm)	0.32 ± 0.06
75:25 poly(HEMA-co-AAm)	0.29 ± 0.02
90:10 poly(HEMA-co-AAm)	0.27 ± 0.01

4.5 Effect of Uric Acid on Phosphorescence Lifetime

After characterizing oxygen response, the effect of uric acid, in a 0 – 10 mg/dL analytical range, on phosphorescence lifetime was investigated. At normal physiological conditions, serum uric acid concentrations typically range from 2.5 to 7.0 mg/dL in men and 1.5 – 6.0 mg/dL in women.[62] Although, uric acid levels vary by individual, the clinical threshold for hyperuricemia is

generally set around the physiological solubility limit of the compound, 6.8 mg/dL.[110] Therefore, the selected analytical range for this system should be well suited for most serum uric acid measurements.

The uric acid test results, illustrated in Figure 4-9, demonstrate an increase in phosphorescence lifetimes with increased uric acid concentration in biosensors of all copolymer compositions. Since the presence of uric acid drives oxygen depletion, reducing oxygen-induced collisional quenching of the phosphorescence lifetime of BMAP; this positive correlation between uric acid concentration and phosphorescence lifetime is expected. The lack of a signal plateau through the specified analytical range indicates that the system is not oxygen or enzyme limited.

Interestingly, when tested with a solution containing no uric acid, the biosensor composed of the 50:50 poly(HEMA-co-AAm) hydrogel has a phosphorescence lifetime roughly 10 µs lower than the other two compositions, implying that the oxygen quenching phenomenon was more pronounced in this composition than in the other two compositions.

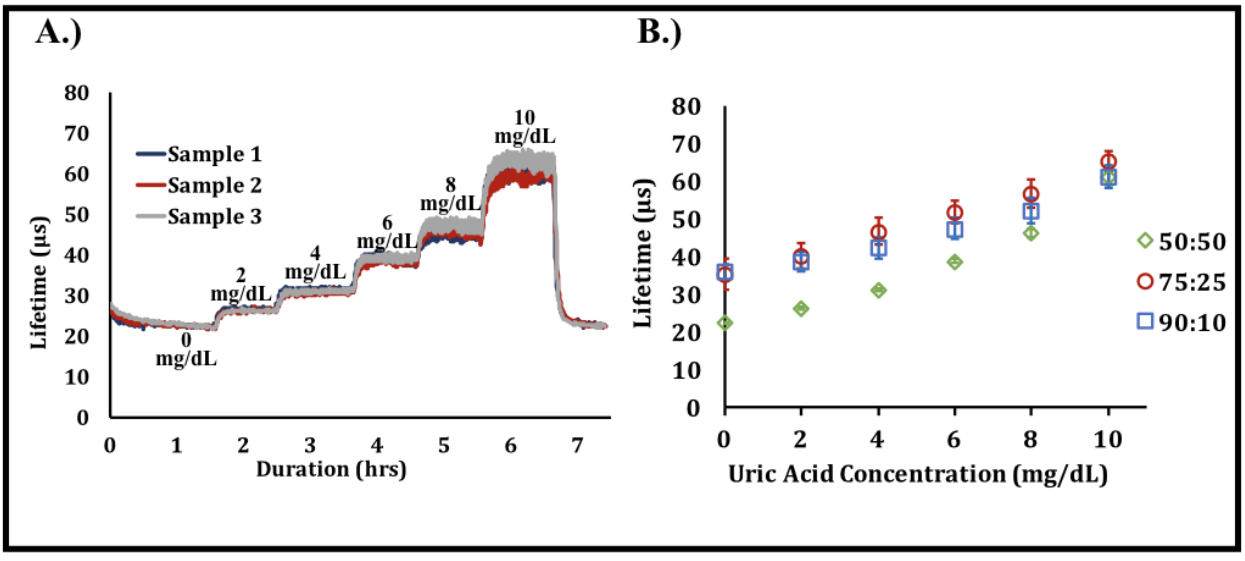

Figure 4-9: (A) Change in phosphorescence lifetime over time (B) Phosphorescence lifetime as a function of uric acid concentration for 3 compositions of poly(HEMA-co-AAm).

This observation is likely due to the increased access of the phosphors to molecular oxygen, due to the higher hydrophilicity of the 50:50 copolymer composition, as indicated by the findings of the oxygen response tests (Section 4.4).

The primary hypothesis being tested in this particular experiment is as follows: as acrylamide concentration is increased, biosensor sensitivity should increase due to greater hydrogel swelling (demonstrated in Section 4.2). Greater hydrogel swelling creates a less tortuous path for uric acid diffusion, which results in an increase in the rate of uric acid influx into the biosensor matrix. The results of the uric acid response test support the stated hypothesis. Specifically, biosensors of higher acrylamide concentrations were mostly more sensitive with lower limits of detections (Table 4-3). Accordingly, biosensors of the 50:50 poly(HEMA-co-AAm) composition possessed the highest uric acid sensitivity and the lowest limit of detection. Conversely, biosensors of the 90:10 composition were the least sensitive, while the 75:25 composition had the lowest limit of detection among the three compositions, which was unexpected. However, since the analytical range was calculated by adding 3 times the standard deviation to the uric acid concentration corresponding to the baseline lifetime (0 mg/dL), the calculated limit of detection of this system is more of a quantification of the sample variation at low uric acid concentrations than a pure metric of uric acid sensitivity.

Table 4-3: Key Metrics for Biosensor Compositions

Composition	LOD (mg/dL)	Sensitivity μs/(mg/dL)
50:50 poly(HEMA-co-AAm)	2.28 ± 1.23	3.71 ± 0.17
75:25 poly(HEMA-co-AAm)	4.01 ± 1.18	2.92 ± 0.36
90:10 poly(HEMA-co-AAm)	3.13 ± 0.72	2.46 ± 0.09

AAm was copolymerized with HEMA primarily to increase the diffusion of uric acid into the biosensor matrix. The importance of this was demonstrated by previous reports by our group, which indicated that the diffusion rate of glucose through polyHEMA hydrogels was 2 orders of magnitude less than the diffusion rate through poly(HEMA-co-AAm) of various compositions.[99] As expected, this reduction in glucose diffusion also reduces biosensor sensitivity. While glucose and uric acid are unique in structure, we anticipate a similar decrease in biosensor sensitivity in pure HEMA biosensors, hence the use of AAm copolymerization in this uric acid biosensing system. In fact, the reduction of biosensor sensitivity would likely be even more pronounced in this uric acid biosensing system for two reasons. Firstly, uric acid has a much lower physiological concentration than glucose, roughly by 2 orders of magnitude. Secondly, the activity of uricase is significantly lower than that of glucose oxidase.[62,111]

Despite the effect of AAm copolymerization on biosensor sensitivity, in prior studies, high concentrations of the monomer were found to lead to inhomogeneous dispersion of the sensing chemistry and phase separation in the hydrogel matrix. As a result, such copolymers suffered from high sample variation and inconsistent results.[52] In more severe cases, dye molecules precipitate into clusters, which could prevent even access of oxygen to the phosphors, and can lead to an artificial inflation of phosphorescence lifetimes. However, this phenomenon was not as pronounced in the uric acid biosensing system described in this report. This may be attributed to the greater amount of enzymes used when compared to glucose sensors, due to the lower activity of the uricase when compared to glucose oxidase. The amphiphilic ability of proteins to easily dissolve in water, while possessing hydrophobic domains that interact with phosphors,[108] likely promotes the even dispersion and solubility of dye within the hydrogel matrix, negating the phase

separation observed in copolymers of high AAm concentrations. This also highlights the importance of proper mixing of the precursor solution prior to crosslinking.

As shown in Figure 4-9, all three copolymer compositions selected in the presented study were well suited for conducting uric acid measurements in a 0 – 10 mg/dL analytical range, with the 50:50 compositions being the most suitable due to its relatively high sensitivity and low analytical range. Interestingly, the slope of the uric acid calibration curve was slightly concaved upward, indicating that the system was more sensitive in environments with higher concentrations of uric acid. Considering that uric acid drives oxygen depletion, the increase in sensitivity is likely a result of the phosphors being more sensitive in low oxygen environment as illustrated in Figure 4-8.

A limitation of this uric acid biosensor system revealed in Figure 4-9 is the limited phosphorescence lifetime rage, particularly when compared to the absolute lifetime range of BMAP. In the presence of no oxygen, the phosphorescence lifetime of BMAP immobilized in a 50:50 poly(HEMA-co-AAm) is about 240 µs. On the other hand, the highest lifetime obtained in the uric acid response test was roughly 61 µs, just 25% of the maximum lifetime in the oxygen response test. This means the oxygen level within the hydrogel matrix of biosensors immersed in 10 mg/dL of uric acid corresponds to ~5% oxygen, as per the oxygen calibration curve of the 50:50 poly(HEMA-co-AAm) hydrogel composition. This reduced oxygen depletion is likely a result of the low enzyme activity of uricase combined with low physiological concentration of uric acid in the human body. To improve the biosensor sensitivity, the oxygen concentration should be closer to 0 to allow for better resolution of changes in uric acid concentration. Theoretically, this can be done by increasing: (1) the activity of uricase through genetic or chemical modifications, (2)

further increasing the mesh size of the hydrogel to improve uric acid diffusion into the hydrogel matrix, (3) conducting the uric acid response tests in *in-vivo*-like low oxygen concentrations.

4.6 Selectivity

A key advantage of using uricase as a bioreceptor its excellent natural selectivity. In most mammals, uricase converts uric acid into allantoin, which is much more soluble in serum. However, to avoid uric acid buildup in the body, humans must excrete the compound, mostly through urine. Interestingly, although humans possess the gene for the uricase, the enzyme is transcriptionally inactive due to an unknown mechanism during primate evolution.[69] In this system, uricase from recombinant Escherichia coli (E. coli) was physically immobilized in the biosensor matrix to specifically detect uric acid, while driving the local depletion of oxygen.

To test the selectivity of the system, the optical response of uric acid biosensors to various physiological concentrations of various organic metabolites commonly found in human serum was reported in Table 4-4. As expected, biosensors were the most sensitive to uric acid, while producing minimal (< 5%) responses to most other alternate analytes. Notable unexpected responses were produced when sensors were exposed to sucrose and glucose, which produced responses equivalent to 18% and 11% of the uric acid response respectively. Neither glucose or sucrose is a known to interfere with uricase function,[112-114] therefore the observed response was more likely as result of an alteration in hydrogel environment or other experimental conditions during sucrose and glucose tests. One possible explanation for this phenomenon is a change in dissolved oxygen in the buffer solution upon the addition of sucrose and glucose, which may affect phosphorescence lifetime. A similar alteration in dissolved oxygen has been noted upon the addition of glucose to cell culture media.[115] To better understand the effect of sucrose and glucose on the response of the uric acid biosensors, additional tests would need to performed.

Table 4-4: Selectivity of Uric Acid Biosensors

	Concentration (mg/dL)	Percent Change
Uric Acid	5	28.92 ± 2.10
Ascorbic Acid	1.8	1.17 ± 0.19
Glucose	90	3.15 ± 2.29
Sucrose	2.7	5.14 ± 3.25
Fructose	0.15	0.99 ± 0.61
Urea	36	0.45 ± 0.13
Allantoin	0.25	1.14 ± 0.61
Creatine	2.6	0.73 ± 0.51
Creatinine	0.9	0.63 ± 0.33
Acetaminophen	0.9	0.48 ± 0.16

4.6 Stability

Maintaining repeatability and stability is of critical importance to the function of long-term implantable biosensors. Drifts in biosensor responses can lead to inaccurate measurements and the administration of the wrong dosage of medication, or the failure to recognize a critical health situation. Enzymatic biosensors in particular are vulnerable to changes in apparent sensitivity over time due to the denaturation and leaching of enzymes. However, the use of hydrogels for enzyme immobilization has been shown to improve enzyme stability,[116] although not in all cases. For instance, certain chemical immobilization techniques introduce conformational changes and steric hindrances that diminish enzyme function.

In the presented uric acid biosensing system, uricase was physically immobilized in a poly(HEMA-co-AAm) copolymer matrix to mitigate bioactivity-loss, while improving enzyme stability.[117,118] However, physical immobilization may come at the cost of increased enzyme leaching due to the lack of chemical bonds with the hydrogel matrix. Another possible source of

signal loss in this system was due to the inactivation of uricase by H_2O_2, a by-product of uric acid catalysis. Therefore, we expected to see a decrease in phosphorescence lifetime in the stability tests. To characterize the stability and repeatability of this system, cyclic stability tests and long-term storage stability tests were used to evaluate the repeatability and stability of the samples *in vitro*, using the previously described flow-through system.

The results of the stability tests yielded mixed results, with cyclic tests showing an unexpected 250% steady increase in phosphorescence lifetime over 20 cycles (Figure 4-10), while the long-term storage tests showed an expected decrease in % response after 8 weeks of storage (Figure 4-11). An analysis of the cyclic stability tests reveals several insights. Firstly, the general increase in lifetime can be observed both when uric acid is present (peaks) and absent (troughs). However, the drift is much more pronounced in the presence of uric acid concentration. A drift at 0 mg/dL uric acid indicates that the drift is not (strictly) a result of changes in enzyme activity or uric acid diffusion but likely due to a change in the hydrogel structure.

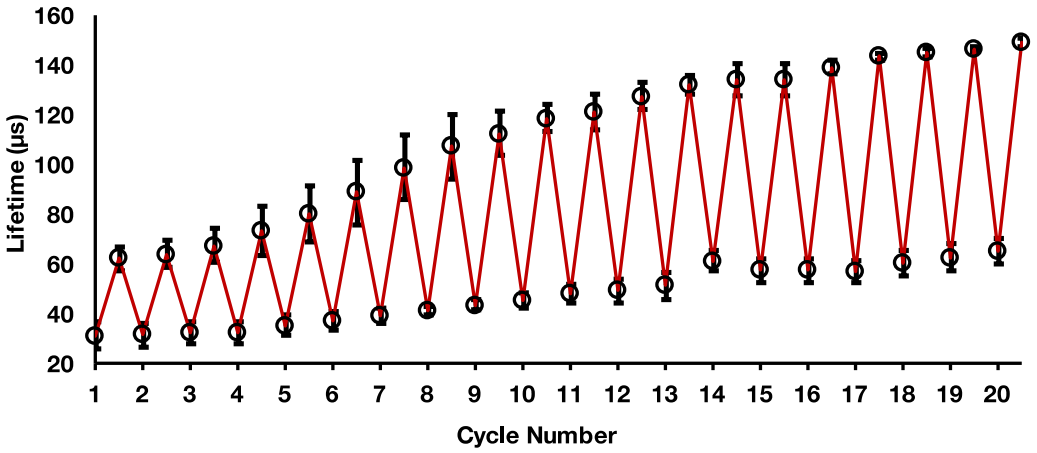

Figure 4-10: Cyclic stability tests

Since the phosphorescence lifetime of BMAP is greater in low oxygen concentrations, these findings imply that oxygen decreases as the number of cycles increase. This increase in lifetime can be the result of a change in the hydrogel structure that increases the interaction

between BMAP and molecular oxygen present in the buffer. A repeat experiment (not shown), similar to the cyclic test illustrated in Figure 4.7 (A), with identical samples was conducted 48 hours after the initial test, demonstrated very similar results to the data show in Figure 4.7 (A). This indicates a reversal in the drift in phosphorescence lifetime and implies that any changes to the hydrogel matrix that may be causing the lifetime increase is reversible, ruling out hydrolytic degradation as the sole cause of this phenomenon.

A more probable cause of the increase phosphorescence lifetime seen in later cycles is due to the weakening of the hydrogen bonds between the carboxyl groups of HEMA and amine groups of AAm due to the elevated temperatures used during testing (37 ℃). Weakned bonds would result in a looser hydrogel network, which may not only allow for easier uric acid diffusion into the biosensor matrix, but better access of dissolved oxygen in the buffer solution to BMAP. Prior studies by Rapado and Peniche detail this temperature-induced breaking of hydrogen bonds in a similar poly(HEMA-co-AAm) hydrogel system in temperatures above 35 ℃.[103]

Results of the storage stability tests, shown in Figure 4-11, indicate that biosensor samples stored in 0 mg/dL uric acid retained 85% of their response, while samples stored in 6 mg/dL uric acid retained 68% of their response after 8 weeks in storage at 23℃. The reduction in biosensor response is likely as result of enzyme leaching and bioactivity loss due to enzyme denaturing over time. H_2O_2 deactivation may also play a role in the reduction of signal retention, as samples stored in a uric acid concentration of 6 mg/dL had a greater reduction in signal retention than samples stored in plain PBS where H_2O_2 production does not occur. However, samples stored in Condition 1 showed an odd trend, where a step decrease in response (week 4) preceded an increase in percent change in lifetime (week 8). Since enzyme denaturing and leaching tends to be irreversible, the trend is less likely a result of a sudden increase in biosensor sensitivity than a result of variations

in sample preparation or other experimental anomalies, such as the samples being punched from a region of low enzyme concentration in the larger hydrogel slab.

This possible sample variation raises a secondary issue in the analysis of the long-term stability of the uric acid biosensors. Specifically, unique samples, punched from different regions of the larger hydrogel slab, were used to represent the different time points (Weeks 1, 4, and 8). As such, the differences in the percent change in phosphorescent lifetime may be a result of, not only the change in biosensor activity over time, but the inherent differences between samples. A low sample variation was assumed during the initial design of these long-term storage stability experiments. To address this oversight, future evaluations of the long-term storage stability of the uric acid biosensors should either use identical samples for long-term stability testing or minimize sample variation and validate this before conducing stability tests using different samples.

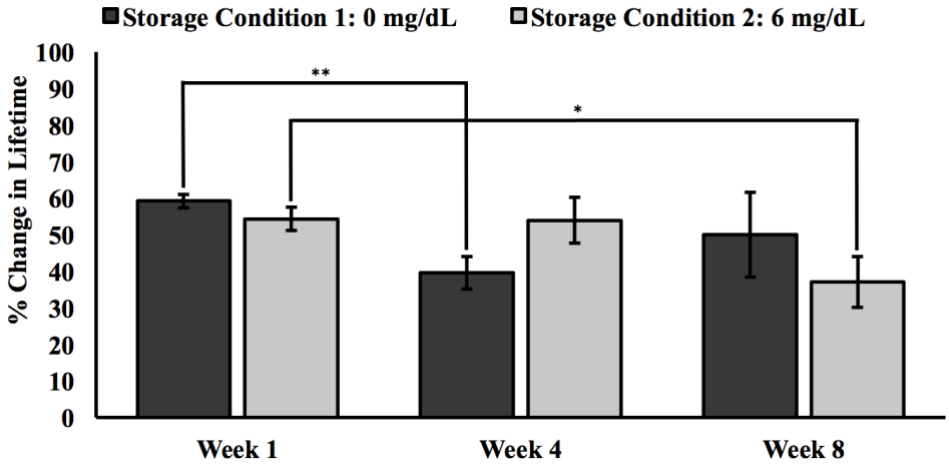

Figure 4-11: Long-term storage stability test

5. SUMMARY AND CONCLUSIONS

5.1 Summary

The surging costs of healthcare, catalyzed by the prevalence of chronic diseases in the aging population, underscores the need for cheaper and better healthcare options. Precision medicine, mobile health, and home health monitoring are emerging as promising initiatives to reduce healthcare costs and improve outcomes of patients who suffer from chronic ailments. Gout, a painful form of arthritis common among geriatric populations, can drastically reduce mobility and quality of life. An on-demand, patient-friendly uric acid biosensor would be valuable in the management of chronic gout. This thesis addressees this challenge through the fabrication and characterization of an optical uric acid biosensor based on oxidoreductase enzymes and oxygen-sensitive phosphors immobilized in a biocompatible hydrogel matrix capable of uric acid monitoring both *in vivo* and *ex vivo*. Upon excitation by red light, samples of these hydrogels produce emission signals with phosphorescence lifetimes proportional to local uric acid concentration. The use of long-lifetime phosphors makes these hydrogels well suited for implantation and transdermal interrogation, with minimal background interference from light absorption, scattering, autofluorescence by the tissue environment.

Three copolymers of HEMA and AAm were tested using a custom *in vitro* flow-through and optical system. The effect of AAm concentration on swelling ratio, oxygen response, and uric acid response were also evaluated. In all compositions, uric acid concentration increased with phosphorescence lifetime in physiologically relevant conditions. Copolymers containing greater concentrations of AAm possessed lower detection limits, higher swelling ratios, and greater uric acid sensitivities, with the 50:50 poly(HEMA-co-AAm) composition being the most ideal for uric

acid biosensing. Conversely, the oxygen sensitivity was nearly identical among the 3 compositions, indicating similar oxygen diffusion rates among the 3 hydrogel types. Evaluations of biosensor selectivity demonstrated the specificity of the system to changes in uric acid concentration, with negligible responses to alternate analytes, with the exception of sucrose and glucose. Finally, biosensor stability tests illuminated some shortcomings of the system. Specifically, an unexpected steady increase in phosphorescence lifetime was observed during cyclic testing. This might indicate an undesired change in the hydrogel matrix during biosensor operation that could affect the long-term function of the system. On the other hand, long-term storage tests showed an 85% retention in the signals of biosensors stored in PBS buffer at 25 ℃ for an 8-week period, and a 68% signal retention in biosensors stored in uric acid solutions at the same temperature and time period.

5.2 Limitations

Overall, this work represents an important but incremental step in the development of an implantable uric acid biosensor for widespread use by gout patients. Looking forward, there are several critical areas that should be addressed to improve the translation of this uric acid biosensing system from benchtop to bedside. The first technical challenge is in the selection a region of implantation. Despite the progress in biosensor research in the past decade, the few implantable biosensors that have progressed from research labs to widespread patient use. Despite the vast possibilities, this class of biosensors have largely been restricted to a few use cases—namely, CGMs implanted in the interstitial space for diabetes management.[37,119] Glucose biosensors are by far the most well established biosensor types.[6] As a result, a plethora of studies on the clinical correlation between serum glucose concentrations and other biofluids, such as interstitial fluid,

sweat, and tears have been published;[29,120,121] although, current implantable glucose biosensors are primarily based on tracking interstitial glucose levels.

Uric acid biosensors on the other hand, do not share this luxury. The clinical literature on the correlation between uric acid concentrations in serum and alternate biofluids, such as interstitial fluid, sweat, tears and saliva are not nearly as vast. Therefore, more clinical studies need be conducted to investigate the correlation between serum uric acid concentrations and alternate biofluids, to enable the design of uric biosensors that do not require blood sampling. Possible regions of implantation to explore include the: synovial spaces, interstitial spaces, and oral cavity. These regions are particularly interesting for uric acid measurements because preliminary studies have shown some correlations between uric acid levels in serum and synovial fluid,[122,123] interstitial fluid,[124-126] and saliva[127,128]—although clinical consensus on these correlations remain elusive. In this pursuit, implantable uric acid biosensors, such as that described in this thesis, can serve as clinical research tools for real-time analysis of uric acid concentrations in various biofluids.

Another limitation of this system is its oxygen dependence. Due to the indirect detection of uric acid through uricase-induced oxygen depletion, unanticipated changes in the molecular oxygen around the sensor can result in erroneous sensor readings. For instance, pathological conditions such as coronary heart disease, stroke, diabetes, and cancer as associated with tissue hypoxia,[129] which might interfere with biosensing. Therefore, an oxygen reference must be used in concert with this system, and changes in oxygen concentration should be compensated for during analysis. Multiplexed uric acid biosensing, using alternate biosensing mechanisms based on the detection of a byproduct of the uric acid-uricase reaction, could be another means to compensate for the oxygen dependence.

5.3 Future Work

During the characterization of this biosensor system, uric acid response tests were conducted in ambient oxygen concentrations (21%). However, typical *in vivo* oxygen concentrations have been reported to be much lower, varying between 1% and 11% oxygen.[129] For the translation of this uric acid biosensing platform from "bench-to-bedside", an in depth characterization of the uric acid response in low oxygen concentrations must be conducted. Doing will likely show the system to be more effective *in vivo*. Since the phosphors are most sensitive at low oxygen, the sensitivity of the system should significantly improve in these conditions. However, drastic oxygen depletion, which is a much greater risk at low oxygen concentrations, might transform the system from being uric acid-limited to oxygen-limited, thereby inhibiting the utility of the system as a uric acid biosensor. If necessary to compensate for the decreased concentration of oxygen, the diffusivity of uric acid into the biosensor matrix can also be decreased by reducing the hydrogel mesh size with the use of lower molecular weight monomers and a higher concentration of crosslinker during hydrogel fabrication.

Improving the cycle repeatability and long-term stability of the uric acid bioresponsive gels is necessary to advance this platform. To address the unexpected drift in phosphorescence lifetime observed after cyclic testing of the biosensors, the effect of temperature on the swelling of the copolymer matrix can be investigated. Alternate hydrogel compositions should be used if poly(HEMA-co-AAm) is found to continuously swell in physiological temperatures. Thermoresponsive polymers, such as poly(N-isopropylacrylamide) (PNIPAAm) are widely studied for their applications in fields like drug delivery and tissue engineering.[130] Interestingly, PNIPAAm-based hydrogels have been used in the development of self-cleaning implantable glucose biosensors by Grunlan and coworkers.[131] However, in the development of this uric acid

biosensing system, unanticipated temperature-induced swelling might be the underlying reason behind the increase in lifetime seen in later test cycles, due to changes in fluid convection and increases in the diffusion of oxygen and uric acid.

Considerations should also be made for the long-term stability of the system. Central to this challenge is the use of enzymes, which are vulnerable to peroxidase deactivation and leaching, both of which can result in reduced biosensor response over time. In future studies, catalase can be used as a hydrogen peroxide scavenger to increase the longevity of the sensor by preventing the deactivation of uricase during long-term use. To reduce the risk of leaching, a small amount of 2-aminoethylmethacrylate (AEMA) can be added to the copolymer and an EDC/NHS [1-ethyl-3-(3-dimethylamino) propyl carbodiimide hydrochloride (EDC)/ N-hydroxysuccinimide (NHS)] reaction can be used to crosslink the carboxyl groups of uricase to the amine groups of AEMA. With uricase crosslinked to the hydrogel matrix and free from peroxidase deactivation, the sensor lifetime will likely significantly increase.

In the development of any implantable biosensor, an important challenge to consider the issue of fibrotic encapsulation of the biosensing component that can obstruct analyte delivery to the biosensor matrix and reduce biosensor sensitivity. A variety of approaches have been explored to mitigate such immune events, such as the use of hydrogels containing zwitterionic materials, hydrophilic polymers, and chemical modifications of the sensor matrix to minimize sensor-foulant interactions.[132,133] However, even with the use of these strategies, host response to sensor implantation remains problematic. A proven strategy to combat this issue would be to embed dexamethasone-loaded poly D,L-lactic-co-glycolic acid (PLGA) microparticles within the hydrogel matrix for the controlled release of the corticosteroid for local immunosuppression.[134]

Dexamethasone is widely used for this purpose, and was successful demonstrated in the use of the first ever, 180-day fully impalpable Eversense XL continuous glucose monitor by Senseonics.[45]

Uric acid is not only relevant to gout management, the compound is also associated with other major chronic diseases like hypertension, stroke, diabetes, and chronic kidney disease.[135-137] Therefore, this biosensing system can be used in concert with other combinations of oxidoreductase enzymes and phosphors in the development of multiplex biosensors for the management or diagnosis of different chronic conditions. Accordingly, work is underway in our group on using 3-d casted poly(ethylene glycol) diacrylate (DA) hydrogel monoliths in the development of "bar code" implantable biosensors, with discrete sensing compartments "coded" with unique combinations of optically responsive assays encapsulated in alginate microparticles to allow for the measurement of different analytes (Figure 5-1). Developing a multianalyte biosensor for the management of chronic kidney disease is most in-line with this work, since renal dysfunction is usually the underlying condition of hyperuricemia.

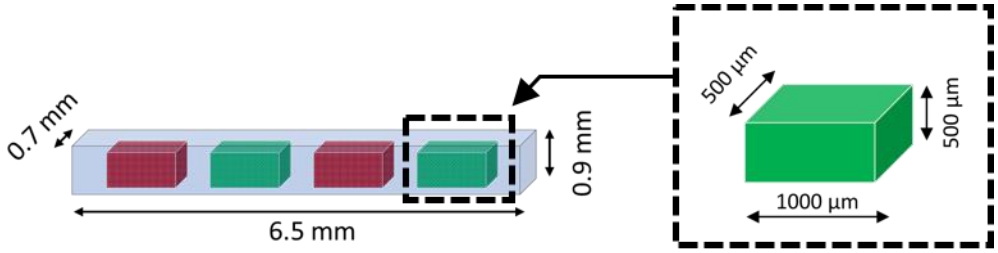

Figure 5-1: Barcode sensors for multiplex biosensing

REFERENCES

1 Crimmins, E. M. Lifespan and Healthspan: Past, Present, and Promise. *Gerontologist* **55**, 901-911, doi:10.1093/geront/gnv130 (2015).

2 Bureau, U. S. C. A Look at the 1940 Census. https://www.census.gov/newsroom/cspan/1940census/CSPAN_1940slides.pdf (2010).

3 Yach, D., Hawkes, C., Gould, C. L. & Hofman, K. J. The Global Burden of Chronic DiseasesOvercoming Impediments to Prevention and Control. *JAMA* **291**, 2616-2622, doi:10.1001/jama.291.21.2616 (2004).

4 Buchan, J. Global nursing shortages. *BMJ* **324**, 751-752, doi:10.1136/bmj.324.7340.751 (2002).

5 Paré, G., Jaana, M. & Sicotte, C. Systematic Review of Home Telemonitoring for Chronic Diseases: The Evidence Base. *Journal of the American Medical Informatics Association* **14**, 269-277, doi:10.1197/jamia.M2270 (2007).

6 Turner, A. P. F. Biosensors: sense and sensibility. *Chemical Society Reviews* **42**, 3184-3196, doi:10.1039/C3CS35528D (2013).

7 Berk, M. L. & Monheit, A. C. The Concentration Of Health Care Expenditures, Revisited. *Health Affairs* **20**, 9-18, doi:10.1377/hlthaff.20.2.9 (2001).

8 Frenk, J., Bobadilla, J. L., SepuúLveda, J. & Cervantes, M. L. Health transition in middle-income countries: new challenges for health care. *Health Policy and Planning* **4**, 29-39, doi:10.1093/heapol/4.1.29 (1989).

9 Kaveeshwar, S. A. & Cornwall, J. The current state of diabetes mellitus in India. *Australas Med J* **7**, 45-48, doi:10.4066/AMJ.2013.1979 (2014).

10 Lahariya, C. & Paul, V. K. Burden, Differentials, and Causes of Child Deaths in India. *The Indian Journal of Pediatrics* **77**, 1312-1321, doi:10.1007/s12098-010-0185-z (2010).

11 Steyn, K., Bradshaw, D., Norman, R. & Laubscher, R. Determinants and treatment of hypertension in South Africans: The first Demographic and Health Survey. *SAMJ: South African Medical Journal* **98**, 376-380 (2008).

12 Gambhir, S. S., Ge, T. J., Vermesh, O. & Spitler, R. Toward achieving precision health. *Science Translational Medicine* **10**, eaao3612, doi:10.1126/scitranslmed.aao3612 (2018).

13 Chiarini, G., Ray, P., Akter, S., Masella, C. & Ganz, A. mHealth Technologies for Chronic Diseases and Elders: A Systematic Review. *IEEE Journal on Selected Areas in Communications* **31**, 6-18, doi:10.1109/JSAC.2013.SUP.0513001 (2013).

14 Patil, S. B., Annese, V. F. & Cumming, D. R. S. in *Advances in Nanosensors for Biological and Environmental Analysis* (eds Akash Deep & Sandeep Kumar) Ch. 8, 133-142 (Elsevier, 2019).

15 Bhalla, N., Jolly, P., Formisano, N. & Estrela, P. Introduction to biosensors. *Essays Biochem* **60**, 1-8, doi:10.1042/EBC20150001 (2016).

16 Trung, T. Q. & Lee, N.-E. Flexible and Stretchable Physical Sensor Integrated Platforms for Wearable Human-Activity Monitoringand Personal Healthcare. *Advanced Materials* **28**, 4338-4372, doi:10.1002/adma.201504244 (2016).

17 Koydemir, H. C. & Ozcan, A. Wearable and Implantable Sensors for Biomedical Applications. *Annual Review of Analytical Chemistry* **11**, 127-146, doi:10.1146/annurev-anchem-061417-125956 (2018).

18 Ledger, D. & McCaffrey, D. Inside wearables: How the science of human behavior change offers the secret to long-term engagement. *Endeavour Partners* **200**, 1 (2014).

19 Thévenot, D. R., Toth, K., Durst, R. A. & Wilson, G. S. Electrochemical biosensors: recommended definitions and classification1International Union of Pure and Applied Chemistry: Physical Chemistry Division, Commission I.7 (Biophysical Chemistry); Analytical Chemistry Division, Commission V.5 (Electroanalytical Chemistry).1. *Biosensors and Bioelectronics* **16**, 121-131, doi:https://doi.org/10.1016/S0956-5663(01)00115-4 (2001).

20 Yoo, E.-H. & Lee, S.-Y. Glucose Biosensors: An Overview of Use in Clinical Practice. *Sensors* **10**, doi:10.3390/s100504558 (2010).

21 Mehrotra, P. Biosensors and their applications – A review. *Journal of Oral Biology and Craniofacial Research* **6**, 153-159, doi:https://doi.org/10.1016/j.jobcr.2015.12.002 (2016).

22 Grieshaber, D., MacKenzie, R., Vörös, J. & Reimhult, E. Electrochemical Biosensors - Sensor Principles and Architectures. *Sensors (Basel, Switzerland)* **8**, 1400-1458, doi:10.3390/s80314000 (2008).

23 Clark, L. C. & Lyons, C. Electrode systems for continuous monitoring in cardiovascular surgery. *Annals of the New York Academy of Sciences* **102**, 29-45 (1962).

24 Nei, L. Some Milestones in the 50-year History of Electrochemical Oxygen Sensor Development. *ECS Transactions* **2**, 33-38, doi:10.1149/1.2409016 (2007).

25 Chen, C. *et al.* Recent advances in electrochemical glucose biosensors: a review. *RSC Advances* **3**, 4473-4491, doi:10.1039/C2RA22351A (2013).

26 Bandodkar, A. J. & Wang, J. Non-invasive wearable electrochemical sensors: a review. *Trends in Biotechnology* **32**, 363-371, doi:https://doi.org/10.1016/j.tibtech.2014.04.005 (2014).

27 Scholten, K. & Meng, E. A review of implantable biosensors for closed-loop glucose control and other drug delivery applications. *International Journal of Pharmaceutics* **544**, 319-334, doi:https://doi.org/10.1016/j.ijpharm.2018.02.022 (2018).

28 Chandra, S., Siraj, S. & Wong, D. K. Y. Recent Advances in Biosensing for Neurotransmitters and Disease Biomarkers using Microelectrodes. *ChemElectroChem* **4**, 822-833, doi:10.1002/celc.201600810 (2017).

29 Thennadil, S. N. *et al.* Comparison of Glucose Concentration in Interstitial Fluid, and Capillary and Venous Blood During Rapid Changes in Blood Glucose Levels. *Diabetes Technology & Therapeutics* **3**, 357-365, doi:10.1089/15209150152607132 (2001).

30 Sen, D. K. & Sarin, G. S. Tear glucose levels in normal people and in diabetic patients. *The British Journal of Ophthalmology* **64**, 693-695, doi:10.1136/bjo.64.9.693 (1980).

31 Aguirre, A. *et al.* Sialochemistry: A Diagnostic Tool? *Critical Reviews in Oral Biology & Medicine* **4**, 343-350, doi:10.1177/10454411930040031201 (1993).

32 Kim, J., Campbell, A. S. & Wang, J. Wearable non-invasive epidermal glucose sensors: A review. *Talanta* **177**, 163-170, doi:https://doi.org/10.1016/j.talanta.2017.08.077 (2018).

33 Yang, Y. & Gao, W. Wearable and flexible electronics for continuous molecular monitoring. *Chemical Society Reviews* **48**, 1465-1491, doi:10.1039/C7CS00730B (2019).

34 Tseng, R. C., Chen, C.-C., Hsu, S.-M. & Chuang, H.-S. Contact-Lens Biosensors. *Sensors (Basel, Switzerland)* **18**, 2651, doi:10.3390/s18082651 (2018).

35 Kim, J., Campbell, A. S., de Ávila, B. E.-F. & Wang, J. Wearable biosensors for healthcare monitoring. *Nature Biotechnology* **37**, 389-406, doi:10.1038/s41587-019-0045-y (2019).

36 Pantelopoulos, A. & Bourbakis, N. G. A survey on wearable sensor-based systems for health monitoring and prognosis. *IEEE Transactions on Systems, Man, and Cybernetics, Part C (Applications and Reviews)* **40**, 1-12 (2010).

37 Gray, M. *et al.* Implantable biosensors and their contribution to the future of precision medicine. *The Veterinary Journal* **239**, 21-29, doi:https://doi.org/10.1016/j.tvjl.2018.07.011 (2018).

38 Ratner, B. D., Hoffman, A. S., Schoen, F. J. & Lemons, J. E. An introduction to materials in medicine. *Biomaterials Science* **484** (1996).

39 Morais, J. M., Papadimitrakopoulos, F. & Burgess, D. J. Biomaterials/Tissue Interactions: Possible Solutions to Overcome Foreign Body Response. *The AAPS Journal* **12**, 188-196, doi:10.1208/s12248-010-9175-3 (2010).

40 Anderson, J. M., Rodriguez, A. & Chang, D. T. Foreign body reaction to biomaterials. *Semin Immunol* **20**, 86-100, doi:10.1016/j.smim.2007.11.004 (2008).

41 Helton, K. L., Ratner, B. D. & Wisniewski, N. A. Biomechanics of the Sensor-Tissue Interface—Effects of Motion, Pressure, and Design on Sensor Performance and Foreign Body Response—Part II: Examples and Application. *Journal of Diabetes Science and Technology* **5**, 647-656, doi:10.1177/193229681100500318 (2011).

42 Helton, K. L., Ratner, B. D. & Wisniewski, N. A. Biomechanics of the Sensor-Tissue Interface—Effects of Motion, Pressure, and Design on Sensor Performance and the Foreign Body Response—Part I: Theoretical Framework. *Journal of Diabetes Science and Technology* **5**, 632-646, doi:10.1177/193229681100500317 (2011).

43 Hermanides, J., Phillip, M. & DeVries, J. H. Current application of continuous glucose monitoring in the treatment of diabetes: pros and cons. *Diabetes Care* **34 Suppl 2**, S197-S201, doi:10.2337/dc11-s219 (2011).

44 Heo, J. Y. & Kim, S.-H. Toward Long-Term Implantable Glucose Biosensors for Clinical Use. *Applied Sciences* **9**, doi:10.3390/app9102158 (2019).

45 Aronson, R., Abitbol, A. & Tweden, K. S. First assessment of the performance of an implantable continuous glucose monitoring system through 180 days in a primarily adolescent population with type 1 diabetes. *Diabetes, Obesity and Metabolism* **21**, 1689-1694, doi:10.1111/dom.13726 (2019).

46 Jafri, R. Z. *et al.* A Three-Way Accuracy Comparison of the Dexcom G5, Abbott Freestyle Libre Pro, and Senseonics Eversense CGM Devices in an Outpatient Study of Subjects with Type 1 Diabetes. *Diabetes* **67**, 14-OR, doi:10.2337/db18-14-OR (2018).

47 Stenvinkel, P. *et al.* Emerging Biomarkers for Evaluating Cardiovascular Risk in the Chronic Kidney Disease Patient: How Do New Pieces Fit into the Uremic Puzzle? *Clinical Journal of the American Society of Nephrology* **3**, 505, doi:10.2215/CJN.03670807 (2008).

48 Barnes, P. J. *et al.* Pulmonary Biomarkers in Chronic Obstructive Pulmonary Disease. *American Journal of Respiratory and Critical Care Medicine* **174**, 6-14, doi:10.1164/rccm.200510-1659PP (2006).

49 Fassett, R. G. *et al.* Biomarkers in chronic kidney disease: a review. *Kidney International* **80**, 806-821, doi:https://doi.org/10.1038/ki.2011.198 (2011).

50 Mascini, M. & Tombelli, S. Biosensors for biomarkers in medical diagnostics. *Biomarkers* **13**, 637-657, doi:10.1080/13547500802645905 (2008).

51 Unruh, R. M. *et al.* Preclinical Evaluation of Poly(HEMA-co-acrylamide) Hydrogels Encapsulating Glucose Oxidase and Palladium Benzoporphyrin as Fully Implantable Glucose Sensors. *J Diabetes Sci Technol* **9**, 985-992, doi:10.1177/1932296815590439 (2015).

52 Andrus, L. P., Unruh, R., Wisniewski, N. A. & McShane, M. J. Characterization of Lactate Sensors Based on Lactate Oxidase and Palladium Benzoporphyrin Immobilized in Hydrogels. *Biosensors (Basel)* **5**, 398-416, doi:10.3390/bios5030398 (2015).

53 Bornhoeft, L. R., Biswas, A. & McShane, M. J. Composite Hydrogels with Engineered Microdomains for Optical Glucose Sensing at Low Oxygen Conditions. *Biosensors (Basel)* **7**, doi:10.3390/bios7010008 (2017).

54 Centers for Disease, C. & Prevention. Prevalence of doctor-diagnosed arthritis and arthritis-attributable activity limitation--United States, 2010-2012. *MMWR Morb Mortal Wkly Rep* **62**, 869-873 (2013).

55 Lawrence, R. C. *et al.* Estimates of the prevalence of arthritis and selected musculoskeletal disorders in the United States. *Arthritis & Rheumatism* **41**, 778-799, doi:10.1002/1529-0131(199805)41:5<778::AID-ART4>3.0.CO;2-V (1998).

56 Sangha, O. Epidemiology of rheumatic diseases. *Rheumatology* **39**, 3-12, doi:10.1093/rheumatology/39.suppl_2.3 (2000).

57 Roddy, E. & Doherty, M. Epidemiology of gout. *Arthritis Res Ther* **12**, 223-223, doi:10.1186/ar3199 (2010).

58 Keenan, R. T. Limitations of the Current Standards of Care for Treating Gout and Crystal Deposition in the Primary Care Setting: A Review. *Clin Ther* **39**, 430-441, doi:10.1016/j.clinthera.2016.12.011 (2017).

59 Wertheimer, A., Morlock, R. & Becker, M. A. A revised estimate of the burden of illness of gout. *Curr Ther Res Clin Exp* **75**, 1-4, doi:10.1016/j.curtheres.2013.04.003 (2013).

60 Edwards, N. L. *et al.* Work productivity loss due to flares in patients with chronic gout refractory to conventional therapy. *Journal of Medical Economics* **14**, 10-15, doi:10.3111/13696998.2010.540874 (2011).

61 Choi, H. K., Mount, D. B. & Reginato, A. M. Pathogenesis of gout. *Annals of Internal Medicine* **143**, 499-516, doi:10.7326/0003-4819-143-7-200510040-00009 (2005).

62 Maiuolo, J., Oppedisano, F., Gratteri, S., Muscoli, C. & Mollace, V. Regulation of uric acid metabolism and excretion. *International Journal of Cardiology* **213**, 8-14, doi:https://doi.org/10.1016/j.ijcard.2015.08.109 (2016).

63 Ghaemi-Oskouie, F. & Shi, Y. The Role of Uric Acid as an Endogenous Danger Signal in Immunity and Inflammation. *Current Rheumatology Reports* **13**, 160-166, doi:10.1007/s11926-011-0162-1 (2011).

64 Martillo, M. A., Nazzal, L. & Crittenden, D. B. The crystallization of monosodium urate. *Curr Rheumatol Rep* **16**, 400, doi:10.1007/s11926-013-0400-9 (2014).

65 Wright, J. D. & Pinto, A. B. Clinical manifestations and treatment of gout. *Primary Care Update for OB/GYNS* **10**, 19-23, doi:https://doi.org/10.1016/S1068-607X(02)00140-3 (2003).

66 Eggebeen, A. T. Gout: an update. *American Family Physician* **76**, 801-808 (2007).

67 Ragab, G., Elshahaly, M. & Bardin, T. Gout: An old disease in new perspective – A review. *Journal of Advanced Research* **8**, 495-511, doi:10.1016/j.jare.2017.04.008 (2017).

68 Fam, A. G. Gout, diet, and the insulin resistance syndrome. *The Journal of Rheumatology* **29**, 1350 (2002).

69 Erden, P. E. & Kilic, E. A review of enzymatic uric acid biosensors based on amperometric detection. *Talanta* **107**, 312-323, doi:10.1016/j.talanta.2013.01.043 (2013).

70 Kim, K. Y., Ralph Schumacher, H., Hunsche, E., Wertheimer, A. I. & Kong, S. X. A literature review of the epidemiology and treatment of acute gout. *Clinical Therapeutics* **25**, 1593-1617, doi:https://doi.org/10.1016/S0149-2918(03)80158-3 (2003).

71 Perez-Ruiz, F., Dalbeth, N. & Bardin, T. A Review of Uric Acid, Crystal Deposition Disease, and Gout. *Advances in Therapy* **32**, 31-41, doi:10.1007/s12325-014-0175-z (2015).

72 Li-Yu, J. *et al.* Treatment of chronic gout. Can we determine when urate stores are depleted enough to prevent attacks of gout? *The Journal of Rheumatology* **28**, 577 (2001).

73 Paraskos, J. *et al.* An analytical comparison between point-of-care uric acid testing meters. *Expert Review of Molecular Diagnostics* **16**, 373-382, doi:10.1586/14737159.2016.1134326 (2016).

74 Zhao, Y., Yang, X., Lu, W., Liao, H. & Liao, F. Uricase based methods for determination of uric acid in serum. *Microchimica Acta* **164**, 1-6, doi:10.1007/s00604-008-0044-z (2009).

75 Lehto, S. Serum uric acid is a strong predictor of stroke in patients with non–insulin-dependent diabetes mellitus. *Stroke* **29**, 635 (1998).

76 George, S. K. *et al.* Improved HPLC method for the simultaneous determination of allantoin, uric acid and creatinine in cattle urine. *Journal of Chromatography B* **832**, 134-137, doi:https://doi.org/10.1016/j.jchromb.2005.10.051 (2006).

77 Galbán, J., Andreu, Y., Almenara, M. J., de Marcos, S. & Castillo, J. R. Direct determination of uric acid in serum by a fluorometric-enzymatic method based on uricase. *Talanta* **54**, 847-854, doi:https://doi.org/10.1016/S0039-9140(01)00335-6 (2001).

78 Villegas, R. *et al.* Purine-rich foods, protein intake, and the prevalence of hyperuricemia: The Shanghai Men's Health Study. *Nutrition, Metabolism and Cardiovascular Diseases* **22**, 409-416, doi:https://doi.org/10.1016/j.numecd.2010.07.012 (2012).

79 Ahmad, R., Tripathy, N., Jang, N. K., Khang, G. & Hahn, Y.-B. Fabrication of highly sensitive uric acid biosensor based on directly grown ZnO nanosheets on electrode surface. *Sensors and Actuators B: Chemical* **206**, 146-151, doi:https://doi.org/10.1016/j.snb.2014.09.026 (2015).

80 Arora, K., Tomar, M. & Gupta, V. Highly sensitive and selective uric acid biosensor based on RF sputtered NiO thin film. *Biosensors and Bioelectronics* **30**, 333-336, doi:https://doi.org/10.1016/j.bios.2011.09.026 (2011).

81 Zhao, Y. *et al.* Highly sensitive uric acid biosensor based on individual zinc oxide micro/nanowires. *Microchimica Acta* **180**, 759-766, doi:10.1007/s00604-013-0981-z (2013).

82 Zhang, Y. *et al.* Development and analytical application of an uric acid biosensor using an uricase-immobilized eggshell membrane. *Biosensors and Bioelectronics* **22**, 1791-1797, doi:https://doi.org/10.1016/j.bios.2006.08.038 (2007).

83 Martinez-Pérez, D., Ferrer, M. L. & Mateo, C. R. A reagent less fluorescent sol–gel biosensor for uric acid detection in biological fluids. *Analytical Biochemistry* **322**, 238-242, doi:https://doi.org/10.1016/j.ab.2003.08.018 (2003).

84 Wang, C.-Y., Huang, C.-W., Wei, T.-T., Wu, M.-Y. & Lin, Y.-W. Fluorescent detection of uric acid in biological samples through the inhibition of cobalt(II) catalyzed Amplex UltraRed. *Sensors and Actuators B: Chemical* **244**, 357-364, doi:https://doi.org/10.1016/j.snb.2017.01.007 (2017).

85 Schrenkhammer, P. & Wolfbeis, O. S. Fully reversible optical biosensors for uric acid using oxygen transduction. *Biosensors and Bioelectronics* **24**, 994-999, doi:https://doi.org/10.1016/j.bios.2008.08.007 (2008).

86 Jin, D. *et al.* Quantitative determination of uric acid using CdTe nanoparticles as fluorescence probes. *Biosensors and Bioelectronics* **77**, 359-365, doi:https://doi.org/10.1016/j.bios.2015.09.057 (2016).

87 Azmi, N. E. *et al.* A simple and sensitive fluorescence based biosensor for the determination of uric acid using H2O2-sensitive quantum dots/dual enzymes. *Biosensors and Bioelectronics* **67**, 129-133, doi:https://doi.org/10.1016/j.bios.2014.07.056 (2015).

88 Liao, L.-T., Liao, C.-C., Liu, C.-C., Yang, T.-Y. & Wang, G.-C. Evaluation of an electrochemical biosensor for uric acid measurement in human whole blood samples. *Clinica Chimica Acta* **436**, 72-77, doi:https://doi.org/10.1016/j.cca.2014.04.033 (2014).

89 Kayamori, Y., Katayama, Y. & Urata, T. Nonenzymatic elimination of ascorbic acid in clinical samples. *Clinical Biochemistry* **33**, 25-29, doi:https://doi.org/10.1016/S0009-9120(99)00082-X (2000).

90 Batumalay, M. *et al.* Tapered plastic optical fiber coated with ZnO nanostructures for the measurement of uric acid concentrations and changes in relative humidity. *Sensors and Actuators A: Physical* **210**, 190-196, doi:https://doi.org/10.1016/j.sna.2014.01.035 (2014).

91 Badugu, R., Lakowicz, J. R. & Geddes, C. D. Ophthalmic glucose monitoring using disposable contact lenses--a review. *Journal of Fluorescence* **14**, 617-633, doi:10.1023/b:jofl.0000039349.89929.da (2004).

92 Misra, N., Kumar, V., Borde, L. & Varshney, L. Localized surface plasmon resonance-optical sensors based on radiolytically synthesized silver nanoparticles for estimation of uric acid. *Sensors and Actuators B: Chemical* **178**, 371-378, doi:https://doi.org/10.1016/j.snb.2012.12.110 (2013).

93 Kant, R., Tabassum, R. & Gupta, B. D. Fiber Optic SPR-Based Uric Acid Biosensor Using Uricase Entrapped Polyacrylamide Gel. *IEEE Photonics Technology Letters* **28**, 2050-2053, doi:10.1109/LPT.2016.2571722 (2016).

94 Borisov, S. M. *et al.* New NIR-emitting complexes of platinum(II) and palladium(II) with fluorinated benzoporphyrins. *Journal of Photochemistry and Photobiology A: Chemistry* **201**, 128-135, doi:https://doi.org/10.1016/j.jphotochem.2008.10.003 (2009).

95 Montheard, J.-P., Chatzopoulos, M. & Chappard, D. 2-Hydroxyethyl Methacrylate (HEMA): Chemical Properties and Applications in Biomedical Fields. *Journal of Macromolecular Science, Part C* **32**, 1-34, doi:10.1080/15321799208018377 (1992).

96 Ratner, B. D. & Hoffman, A. S. in *Hydrogels for Medical and Related Applications* Vol. 31 *ACS Symposium Series* Ch. 1, 1-36 (American Chemical Society, 1976).

97 Rapado, M. & Peniche, C. Synthesis and characterization of pH and temperature responsive poly(2-hydroxyethyl methacrylate-co-acrylamide) hydrogels. *Polímeros* **25**, 547-555 (2015).

98 Dušek, K. & Janáček, J. Hydrophilic gels based on copolymers of 2-hydroxyethyl methacrylate with methacrylamide and acrylamide. *Journal of Applied Polymer Science* **19**, 3061-3075, doi:10.1002/app.1975.070191111 (1975).

99 Roberts, J. R., Park, J., Helton, K., Wisniewski, N. & McShane, M. J. Biofouling of polymer hydrogel materials and its effect on diffusion and enzyme-based luminescent glucose sensor functional characteristics. *J Diabetes Sci Technol* **6**, 1267-1275, doi:10.1177/193229681200600605 (2012).

100 Clark, E. S. Delrin material characteristics. *J Heart Valve Dis* **5 Suppl 2**, S184-189 (1996).

101 Morita, S. Hydrogen-bonds structure in poly(2-hydroxyethyl methacrylate) studied by temperature-dependent infrared spectroscopy. *Front Chem* **2**, 10-10, doi:10.3389/fchem.2014.00010 (2014).

102 YÜRÜKSOY, B. I. Swelling behavior of acrylamide-2-hydroxyethyl methacrylate hydrogels. *Turkish Journal of Chemistry* **24**, 147-156 (2000).

103 Bocourt, M., Bada, N., Acosta, N., Bucio, E. & Peniche, C. Synthesis and characterization of novel pH-sensitive chitosan-poly(acrylamide-co-itaconic acid) hydrogels. *Polymer International* **63**, 1715-1723, doi:10.1002/pi.4699 (2014).

104 Yasuda, K., Okajima, K. & Kamide, K. Study on Alkaline Hydrolysis of Polyacrylamide by 13C NMR. *Polymer Journal* **20**, 1101-1107, doi:10.1295/polymj.20.1101 (1988).

105 Staudinger, C. & Borisov, S. M. Long-wavelength analyte-sensitive luminescent probes and optical (bio)sensors. *Methods and Applications in Fluorescence* **3**, 042005, doi:10.1088/2050-6120/3/4/042005 (2015).

106 Imran, M., Ramzan, M., Qureshi, K. A., Khan, A. M. & Tariq, M. Emerging Applications of Porphyrins and Metalloporphyrins in Biomedicine and Diagnostic Magnetic Resonance Imaging. *Biosensors* **8**, doi:10.3390/bios8040095 (2018).

107 Quaranta, M., Borisov, S. M. & Klimant, I. Indicators for optical oxygen sensors. *Bioanalytical Reviews* **4**, 115-157, doi:10.1007/s12566-012-0032-y (2012).

108 Vinogradov, S. A. & Wilson, D. F. Metallotetrabenzoporphyrins. New phosphorescent probes for oxygen measurements. *Journal of the Chemical Society, Perkin Transactions 2*, 103-111, doi:10.1039/P29950000103 (1995).

109 Niedermair, F. *et al.* Tunable Phosphorescent NIR Oxygen Indicators Based on Mixed Benzo- and Naphthoporphyrin Complexes. *Inorganic Chemistry* **49**, 9333-9342, doi:10.1021/ic100955z (2010).

110 Chhana, A., Lee, G. & Dalbeth, N. Factors influencing the crystallization of monosodium urate: a systematic literature review. *BMC Musculoskeletal Disorders* **16**, 296, doi:10.1186/s12891-015-0762-4 (2015).

111 Güemes, M., Rahman, S. A. & Hussain, K. What is a normal blood glucose? *Archives of Disease in Childhood* **101**, 569, doi:10.1136/archdischild-2015-308336 (2016).

112 Holmberg, C. G. Uricase purification and properties. *Biochem J* **33**, 1901-1906, doi:10.1042/bj0331901 (1939).

113 Machida, Y. & Nakanishi, T. Purification and Properties of Uricase from Enterobacter cloacae. *Agricultural and Biological Chemistry* **44**, 2811-2815, doi:10.1271/bbb1961.44.2811 (1980).

114 Liu, J., Li, G. X., Liu, H. & Zhou, X. Purification and Properties of Uricase from Candida Sp. and Its Application in Uric Acid Analysis in Serum. *Annals of the New York Academy of Sciences* **750**, 477-481, doi:10.1111/j.1749-6632.1995.tb20000.x (1995).

115 Vendruscolo, F. *et al.* Determination of Oxygen Solubility in Liquid Media. *ISRN Chemical Engineering* **2012**, 5, doi:10.5402/2012/601458 (2012).

116 Brady, D. & Jordaan, J. Advances in enzyme immobilisation. *Biotechnology Letters* **31**, 1639, doi:10.1007/s10529-009-0076-4 (2009).

117 Teles, F. R. R. & Fonseca, L. P. Applications of polymers for biomolecule immobilization in electrochemical biosensors. *Materials Science and Engineering: C* **28**, 1530-1543, doi:https://doi.org/10.1016/j.msec.2008.04.010 (2008).

118 Zhang, D.-H., Yuwen, L.-X. & Peng, L.-J. Parameters affecting the performance of immobilized enzyme. *Journal of chemistry* **2013** (2013).

119 Konstantas, D. *An overview of wearable and implantable medical sensors*. Vol. 16 (2007).

120 Moyer, J., Wilson, D., Finkelshtein, I., Wong, B. & Potts, R. Correlation Between Sweat Glucose and Blood Glucose in Subjects with Diabetes. *Diabetes Technology & Therapeutics* **14**, 398-402, doi:10.1089/dia.2011.0262 (2012).

121 Baca, J. T., Finegold, D. N. & Asher, S. A. Tear Glucose Analysis for the Noninvasive Detection and Monitoring of Diabetes Mellitus. *The Ocular Surface* **5**, 280-293, doi:https://doi.org/10.1016/S1542-0124(12)70094-0 (2007).

122 Pascual, E., Batlle-Gualda, E., Martínez, A., Rosas, J. & Vela, P. Synovial Fluid Analysis for Diagnosis of Intercritical Gout. *Annals of Internal Medicine* **131**, 756-759, doi:10.7326/0003-4819-131-10-199911160-00007 (1999).

123 Cajori, F. A., Crouter, C. Y. & Pemberton, R. THE PHYSIOLOGY OF SYNOVIAL FLUID. *JAMA Internal Medicine* **37**, 92-101, doi:10.1001/archinte.1926.00120190095008 (1926).

124 Patterson, R. A., Horsley, E. T. & Leake, D. S. Prooxidant and antioxidant properties of human serum ultrafiltrates toward LDL important role of uric acid. *Journal of Lipid Research* **44**, 512-521 (2003).

125 Mei, D. A., Gross, G. J. & Nithipatikom, K. Simultaneous Determination of Adenosine, Inosine, Hypoxanthine, Xanthine, and Uric Acid in Microdialysis Samples Using Microbore Column High-Performance Liquid Chromatography with a Diode Array Detector. *Analytical Biochemistry* **238**, 34-39, doi:https://doi.org/10.1006/abio.1996.0246 (1996).

126 Kono, H., Chen, C.-J., Ontiveros, F. & Rock, K. L. Uric acid promotes an acute inflammatory response to sterile cell death in mice. *J Clin Invest* **120**, 1939-1949, doi:10.1172/JCI40124 (2010).

127 Soukup, M. *et al.* Salivary uric acid as a noninvasive biomarker of metabolic syndrome. *Diabetology & Metabolic Syndrome* **4**, 14, doi:10.1186/1758-5996-4-14 (2012).

128 Shibasaki, K., Kimura, M., Ikarashi, R., Yamaguchi, A. & Watanabe, T. Uric acid concentration in saliva and its changes with the patients receiving treatment for hyperuricemia. *Metabolomics* **8**, 484-491 (2012).

129 Carreau, A., Hafny-Rahbi, B. E., Matejuk, A., Grillon, C. & Kieda, C. Why is the partial oxygen pressure of human tissues a crucial parameter? Small molecules and hypoxia. *Journal of Cellular and Molecular Medicine* **15**, 1239-1253, doi:10.1111/j.1582-4934.2011.01258.x (2011).

130 Klouda, L. & Mikos, A. G. Thermoresponsive hydrogels in biomedical applications. *European Journal of Pharmaceutics and Biopharmaceutics* **68**, 34-45, doi:https://doi.org/10.1016/j.ejpb.2007.02.025 (2008).

131 Abraham, A. A., Fei, R., Coté, G. L. & Grunlan, M. A. Self-Cleaning Membrane to Extend the Lifetime of an Implanted Glucose Biosensor. *ACS Applied Materials & Interfaces* **5**, 12832-12838, doi:10.1021/am4040653 (2013).

132 Mi, L. & Jiang, S. Integrated Antimicrobial and Nonfouling Zwitterionic Polymers. *Angewandte Chemie International Edition* **53**, 1746-1754, doi:10.1002/anie.201304060 (2014).

133 Wang, Y., Papadimitrakopoulos, F. & Burgess, D. J. Polymeric "smart" coatings to prevent foreign body response to implantable biosensors. *Journal of Controlled Release* **169**, 341-347, doi:https://doi.org/10.1016/j.jconrel.2012.12.028 (2013).

134 Ward, W. K. *et al.* Controlled release of dexamethasone from subcutaneously-implanted biosensors in pigs: localized anti-inflammatory benefit without systemic effects. *J Biomed Mater Res A* **94**, 280-287, doi:10.1002/jbm.a.32651 (2010).

135 Feig, D. I., Kang, D.-H. & Johnson, R. J. Uric acid and cardiovascular risk. *N Engl J Med* **359**, 1811-1821, doi:10.1056/NEJMra0800885 (2008).

136 Johnson, R. J. *et al.* Uric acid and chronic kidney disease: which is chasing which? *Nephrology Dialysis Transplantation* **28**, 2221-2228, doi:10.1093/ndt/gft029 (2013).

137 Dehghan, A., van Hoek, M., Sijbrands, E. J. G., Hofman, A. & Witteman, J. C. M. High Serum Uric Acid as a Novel Risk Factor for Type 2 Diabetes. *Diabetes Care* **31**, 361, doi:10.2337/dc07-1276 (2008).